

Review

Towards higher- T_c superconductors

By Jun AKIMITSU^{*1,*2,†}

(Communicated by Sumio IJIMA, M.J.A.)

Abstract: New superconductors discovered in the Akimitsu laboratory are reviewed here. These materials can be categorized into two groups:

- 1) Cu-oxide superconductors.
 - 1-1 Cu-oxide system having CuO_2 planes.
 - 1-2 Ladder lattice superconductor.
- 2) Exploration of new metal-based superconductors.
 - 2-1 MgB_2 and its application.
 - 2-2 Y_2C_3 .
 - 2-3 Carrier-doped wide-gap semiconductors.
 - 2-4 New superconductor with a cage-type structure: $\text{R}_5\text{T}_6\text{Sn}_{18}$ ($\text{R} = \text{Sc}, \text{Y}, \text{Lu}; \text{T} = \text{Rh}, \text{Ir}$).

Finally, all of the new superconductors discovered in our laboratory are summarized. The outlook for the high- T_c superconductors and our present work are also described.

Keywords: high- T_c superconductors, Cu-oxide system, ladder superconductor, MgB_2 , doped semiconductors, Ir oxide

1. Superconductivity and its applications

Superconductivity was discovered in mercury (Hg) by Kamerlingh Onnes of Leiden University in 1911 ($T_c = 4.2\text{K}$). That was three years after the great achievement of helium (He) liquefaction.

The three major characteristics of superconductivity are first pointed out, and then each of them is explained briefly. They are:

- (1) Zero electrical resistance (a current will persist indefinitely) ($\mathbf{E} = 0$),
- (2) The Meissner effect ($\mathbf{B} = 0$),
- (3) The Josephson effect.

(1) Zero electrical resistance. It is well known that many free electrons exist in metals, and that an electric current is a flow of those electrons. In general, electrons are scattered by the oscillations of atoms (phonons), or by impurities in metals. This can be described by Ohm's law. Since all metal contains

impurities, and atoms oscillate, electrons are always being scattered. Thus, it seems to be impossible to ever experience zero electrical resistance. However, zero electrical resistance actually exists under superconductivity. It can thus be concluded that if an electric current is initiated in a circular superconductor, it would continue to flow indefinitely. This is a totally mysterious phenomenon and it is a puzzle that motivates many physicists to understand. Its final solution was offered by three physicists, (Bardeen, Cooper and Shrieffer), which is now known as the BCS theory.

There may be many applications of the phenomenon of zero electrical resistance, such as superconducting magnets, superconducting power transmission, and electricity storage. For example, there is a grand plan to set up global networks of electric power plants using wind-power generation, or solar batteries in deserts or waste land, and to send electricity generated in these plants to remote urban areas through superconducting cables.

Another example is linear-motor cars that run by 'floating their bodies', using the repulsive power of magnetic fields generated by superconducting magnets.

(2) The Meissner effect. In addition to zero

^{*1} Research Institute for Interdisciplinary Science, Okayama University, Okayama, Japan.

^{*2} Professor Emeritus, Aoyama Gakuin University, Tokyo, Japan.

[†] Correspondence should be addressed: J. Akimitsu, Research Institute for Interdisciplinary Science, Okayama University, 3-1-1 Tsushimanaka, Kita-ku, Okayama 700-8530, Japan (e-mail: akimitsu@okayama-u.ac.jp).

electrical resistance, superconductivity has another unique characteristic. Superconductors have no internal magnetic flux or no lines of magnetic force within their substance ($\mathbf{B} = 0$). This phenomenon is called the Meissner effect, named after its discoverer, which may have many applications, such as magnetic shielding, magnetic levitation, magnetic bearings, and so on.

(3) The Josephson effect. The third major characteristic of superconductivity is the Josephson effect. This is a phenomenon where superconducting electrons flow through between two superconductors separated by a thin barrier, without any voltage being applied. It is a quite unique phenomenon, causing superconducting electrons to flow without a voltage to drive them (DC Josephson effect) or AC current to flow when a DC voltage is applied (AC Josephson effect). In 1962, Josephson, at that time a graduate student at Cambridge University, predicted this phenomenon, specific to superconductivity, that would be a macroscopic effect of quantum mechanics. The most significant application is in a superconducting quantum interference device (SQUID). This may be used in magnetic-field sensors or super high-speed computing machines in the future.

Thus, superconductivity is not only wide and deep as fundamental aspect of physics, but also extremely important concerning applications, and it is expected to be a key to such issues as solving 'Energy problem'. It is no exaggeration to say The 21st century is a century of superconductivity.

2. History of superconductivity exploration— before the discovery of copper oxide superconductors

As mentioned above, superconductivity is a very interesting study area, and has many possible applications. The most serious difficulty, however, is that the superconducting state is only achieved below a certain temperature, the critical temperature (T_c), which is usually very low. Nb_3Ge was a substance with the highest critical temperature obtained by 1980, at 22 K. B.T. Matthias wrote that a room-temperature superconductor is only pure science fiction. However, many scientists have continuously attempted to find superconductors with a higher T_c , and I was one of those people.

The next problem concerns what guiding principles are required to produce a higher T_c ? The only clue is an equation for the superconducting transition temperature based on the BCS theory. According to the simplest BCS theory, the superconducting

transition temperature (T_c) can be expressed as follows:

$$T_c \cong \Theta_D \exp\left(-\frac{1}{\lambda}\right), \quad [1]$$

$$\lambda = N(0) \cdot V, \quad [2]$$

where Θ_D is the Debye temperature, $N(0)$ is the state density on the Fermi surface in the normal conducting state, and V is the size of the electron-phonon interaction.

The parameters that may be easily controlled are the Debye temperature, Θ , and $N(0)$. Matthias focused on substances having a high $N(0)$ (the Matthias Rule). Upon systemic exploration of substances by this method, however, a breakthrough concerning the upper limit of T_c could not be obtained. Therefore, we focused on substances with a large electron-phonon interaction, V . However, when the electron-phonon interaction is increased steadily, electrons are combined in real space, form pairs in real space and stop moving, which becoming insulators. These are called charge density wave (CDW) type insulators. Figure 1 shows a schematic phase diagram, T_c vs. size of the electron-phonon interaction, V . Conversely, can we obtain superconductors with a high T_c if we decrease the electron-phonon coupling constant, V , of the charge density wave-type insulators? Based on this idea, we discovered that $\text{Nb}_{1-x}\text{Ta}_x\text{Se}_3$ became a superconductor when $T_c = 4$ K, by substituting the Ta at the Nb site to the CDW material, NbSe_3 to form $\text{Nb}_{1-x}\text{Ta}_x\text{Se}_3$ and reducing V ¹⁾ (Fig. 2).

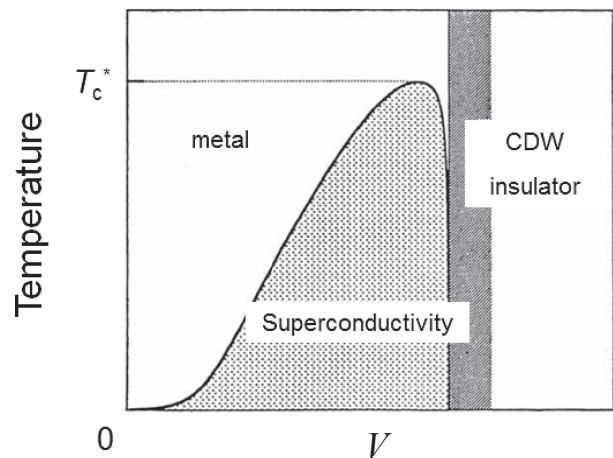


Fig. 1. Phase diagram of the electron-phonon coupling constant V vs. superconducting critical temperature T_c . (N. Tsuda, K. Nasu, J. Fujimori and K. Siratori: *Electronic Conduction in Oxide* (in Japanese) p. 120.).

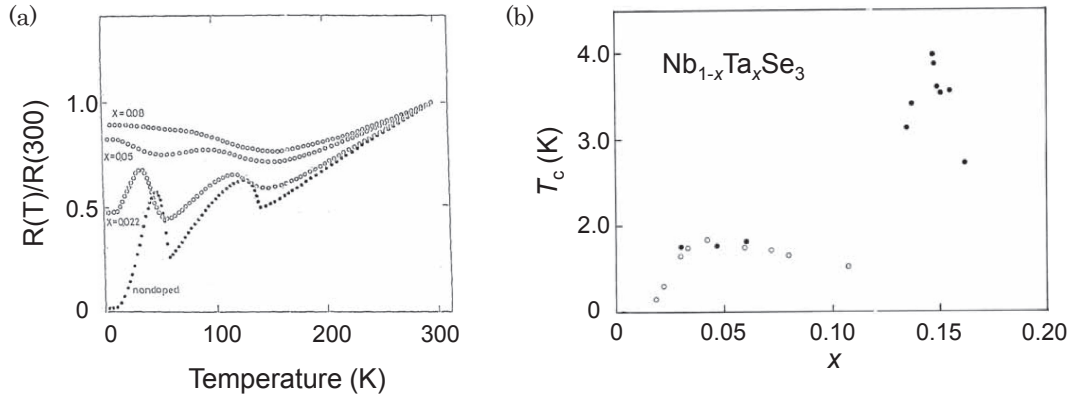


Fig. 2. (a) Normalized resistance as a function of the temperature for $Nb_{1-x}Ta_xSe_3$ with several Ta concentrations. (b) Ta concentration dependence of T_c . Substituting Ta to CDW material $NbSe_3$, forming $Nb_{1-x}Ta_xSe_3$ to be superconductive.¹⁾ ○ K. Kawabata,²⁾ ● Our data.¹⁾

3. Discovery of copper oxide superconductors

3-1. New Cu-oxide system having CuO_2 planes. Meanwhile, Bednorz and Müller discovered copper oxide superconductors (1986).³⁾ The substance they found was an oxide, called La–Ba–Cu–O. It is said that they first noticed that crystals were distorted because Cu^{2+} was a Jahn-Teller ion, and they supposed that a high T_c might be obtained by changing the static distortion to a dynamic charge fluctuation. This is very similar to our idea. After that discovery, many groups figured out that this substance was two-dimensional, and that T_c was quickly increased to 160 K just a few years later.

This “revolution within the history of science” eliminated the widely accepted major prejudice that superconductivity is only possible in non magnetic materials. Leaving to other books the dramatic historical details of how a small bud germinated by Bednorz and Müller blossomed into a mainstream concept, here we describe what I did during this period. It is well known that after Bednorz and Müller discovered superconductivity in a copper oxide, a group led by Paul Chu found $YBa_2Cu_3O_y$ (YBCO).⁴⁾ Around that time, I started studying the Cu-oxide system in earnest. My idea of how to create a new superconductor centered on the radius of ions. As shown in Table 1, I noticed that all ionic radii of elements in superconductors obtained until then were in the vicinity of 1 Å. Are there any other elements with ionic radii in that vicinity? I found that only four such ions exist: Bi^{3+} , Tl^{3+} , Hg^{2+} , and Cd^{2+} , as listed in Table 1. Surprisingly, these elements (except for Cd), were components of Bi-based, Tl-based, and Hg-based superconductors with a higher T_c .

Table 1. Ionic radius around 1 Å. Upper part ($Ca^{2+} \sim Y^{3+}$) shows the elements, being composed of La-Sr(Ba)-Cu-O and Y-Ba-Cu-O systems. Lower part ($Bi^{3+} \sim Cd^{2+}$) is the expected elements. Later, these elements Bi^{3+} , Tl^{3+} and Hg^{2+} are composed of the high- T_c superconductors, called Bi-, Tl- and Hg-systems

Cation	Ionic radius [Å] (6-coordination)
Ca^{2+}	1.02
Sr^{2+}	1.18
Ba^{2+}	1.38
Y^{3+}	0.91
La^{3+}	1.08

Bi^{3+}	1.04
Tl^{3+}	1.08
Hg^{2+}	1.04
Cd^{2+}	0.97

We now describe here some successful and unsuccessful stories. At that time, we started with the combination of Bi–Sr–Cu–O suggested by Table 1, and immediately obtained a superconductor with $T_c = 6$ K. Figure 3 shows its crystal structure and electrical resistance.^{5),6)} In a search of superconductors with a higher T_c , we replaced Nd^{3+} , *etc.* with different valences at the site of Sr^{2+} for carrier doping. We then found signs of superconductors with $T_c = 50$ K, and were excitedly working on its single-phase formation. Meanwhile we heard about the discovery of Bi–Sr–Ca–Cu–O with $T_c = 77$ K and $T_c = 105$ K by Maeda *et al.*⁷⁾ I was disappointed by this discovery, because when one of my students tried to replace Sr^{2+} with Ca^{2+} , I did not agree with his idea, because Sr^{2+} and Ca^{2+} are both divalent elements, and they would only dissolve, leading to

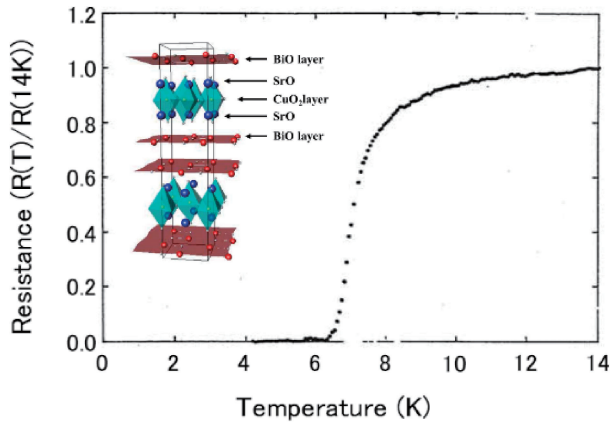


Fig. 3. Temperature dependence of resistance in $\text{Bi}_2\text{Sr}_2\text{CuO}_6$. The inset shows the crystal structure.⁵⁾

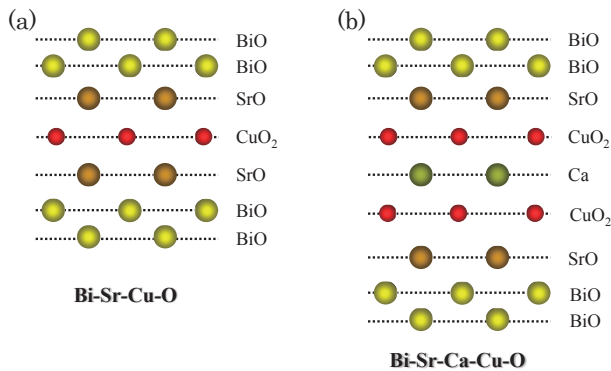


Fig. 4. Layered structure of (a) $\text{Bi}_2\text{Sr}_2\text{CuO}_6$ and (b) $\text{Bi}_2\text{Sr}_2\text{CaCu}_2\text{O}_8$.

nothing interesting chemically. However, it became clear that, in fact, when Sr and Ca are mixed, they enter into completely different sites due to their different ionic radii, resulting in different crystal structures (Fig. 4).

Here is another example of our successful and unsuccessful cases. There is a substance, $\text{Nd}_2\text{CuO}_{4-\delta}$, called a fluorite type structure, whose structure was known at that time. Unlike La_2CuO_4 , it does not have oxygen above and below the copper in its crystal structure. We figured out that this substance became metallic when Ce^{4+} was replaced with Nd^{3+} . Then, one of my students suggested, “let’s mix in Sr^{2+} in addition to Ce^{4+} ”. But I objected to this idea, saying that the number of carriers might be canceled if Sr^{2+} was mixed with Ce^{4+} . But I remembered my previous mistake, and agreed to try this idea, in fact, a superconductor with a totally new structure emerged.^{8),9)} Figure 5 shows its crystal structure (called “ T^* structure”) and electrical resistivity.

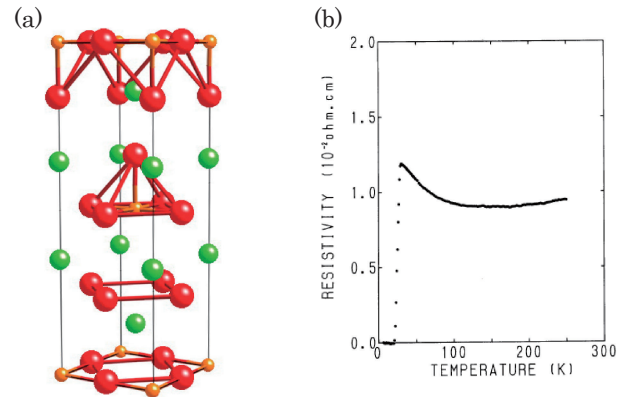


Fig. 5. Superconductivity in $(\text{Nd}, \text{Sr}, \text{Ce})_2\text{CuO}_4$: T^* structure. (a) Crystal structure of T^* structure. (b) Temperature dependence of resistivity in T^* structure.^{8),9)}

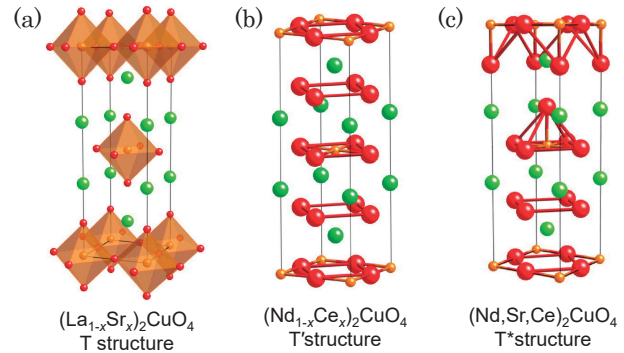


Fig. 6. Three types of “214” structure: (a) $(\text{La}_{1-x}\text{Sr}_x)_2\text{CuO}_4$: T structure, (b) $(\text{Nd}_{1-x}\text{Ce}_x)_2\text{CuO}_4$: T' structure, (c) $(\text{Nd}, \text{Sr}, \text{Ce})_2\text{CuO}_4$: T^* structure.

Shortly after that, however, Tokura *et al.* discovered a new type of superconductor,¹⁰⁾ an electron-doped type, by reducing the oxygen in $(\text{Nd}_{1-x}\text{Ce}_x)_2\text{CuO}_4$. This is called the T' structure. Figure 6 shows the “214”-type crystal structure with a different coordination having a CuO_2 plane.

Meanwhile, some essential characteristics of copper oxide superconductors had become clear.

1. The first is the existence of a CuO_2 plane consisting of Cu and O. This “parent compound” is both antiferromagnetic and insulating at the same time. This is called a Mott insulator.

2. The second characteristic is that a superconductor emerges after holes or electrons are introduced into this Mott insulator, and electricity starts flowing. Block layers adhere to the CuO_2 plane and adjust the electric charges. Figure 7 is a schematic diagram of these block layers.¹¹⁾ Superconductors with different T_c are generated by replacing these block layers.

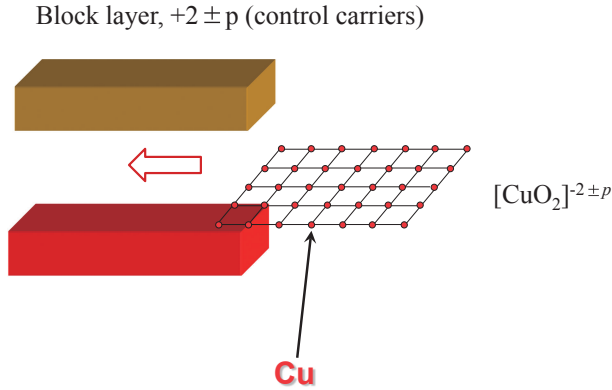


Fig. 7. Concept of the block layer. CuO_2 layers are inserted between block layers.¹¹⁾

The next logical step is to assemble new superconductors using these block layers. This idea is specifically to create new superconductors by finding

new block layers, and combining them with existing block layers. For example, there is a substance with the crystal structure $\text{Sr}_2\text{CuO}_2(\text{CO}_3)$.¹²⁾ This is a new copper oxide that includes a carbonate group, but this is not a superconductor itself. What should be done to dope this with a carrier? One of my doctor-course students, Masatomo Uehara (currently Yokohama National University), came up with an interesting method. It was to replace CO_3^{-2} with BO_3^{-3} , and thus effectively inject a carrier, and generating a new superconductor, $\text{Sr}_2\text{CuO}_2(\text{CO}_3)_{1-x}(\text{BO}_3)_x$.¹³⁾ Figure 8 shows a phase diagram with the boron content x vs. temperature in $\text{Sr}_2\text{CuO}_2(\text{CO}_3)_{1-x}(\text{BO}_3)_x$. This superconductor is a new copper oxide that includes a carbonate group. Is it possible to create a new type superconductor by combining this crystal structures and those of existing superconductors? It was not as easy as it sounds, but we finally were able to synthesize a

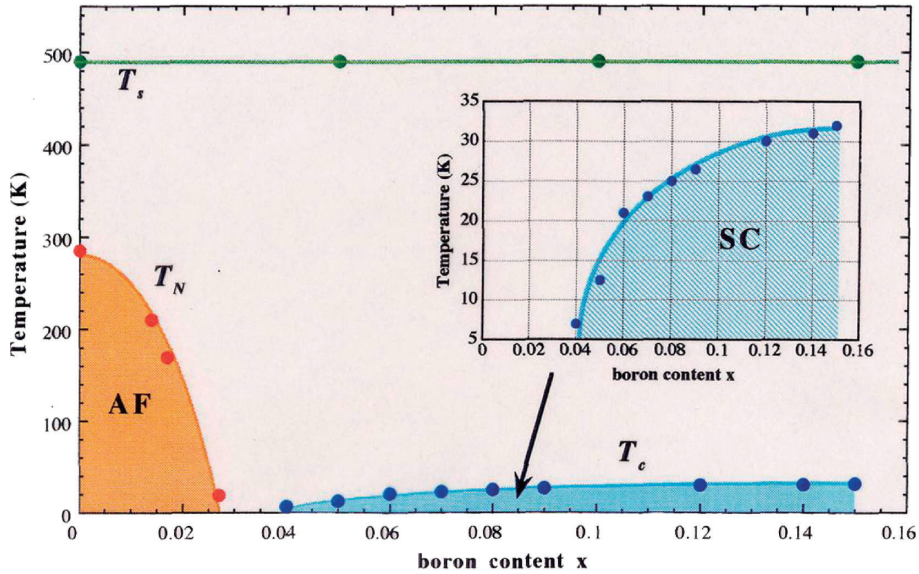


Fig. 8. Phase diagram of $\text{Sr}_2\text{CuO}_4(\text{CO}_3)_{1-x}(\text{BO}_3)_x$. Carriers can be controlled by (BO_3) content.¹³⁾

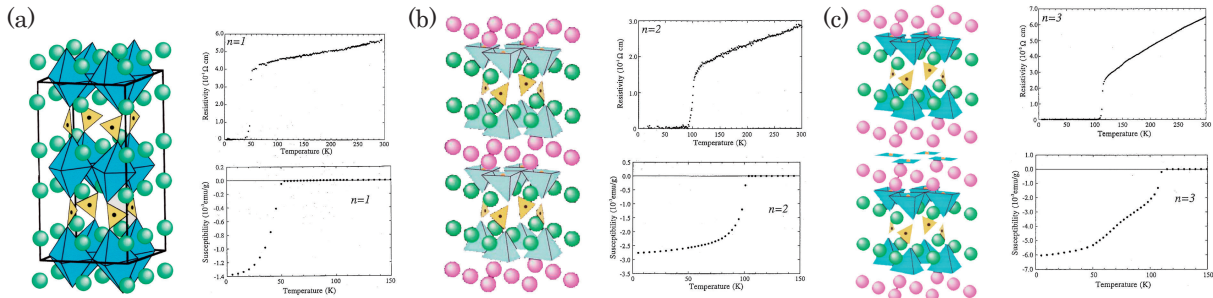


Fig. 9. Three types of superconductor composed of different block layers including the carbonate layers. (a) $\text{Sr}_2\text{CuO}_2(\text{CO}_3)_{1-x}(\text{BO}_3)_x$ ($T_c = 55$ K) (b) $\text{Sr}_2\text{CaCu}_2\text{O}_4(\text{CO}_3)_{1-x}(\text{BO}_3)_x$ ($T_c = 105$ K) (c) $\text{Sr}_2\text{Ca}_2\text{CuO}_4(\text{CO}_3)_{1-x}(\text{BO}_3)_x$ ($T_c = 115$ K).¹⁵⁾

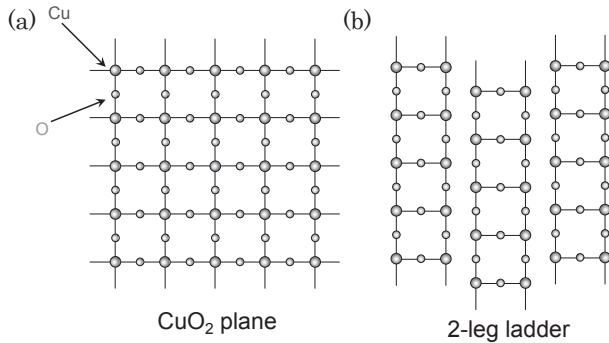


Fig. 10. Two types of Cu-O planes. (a) Two-dimensional CuO_2 planes, (b) Two-leg ladder Cu_2O_3 planes.

new superconductor under high pressure. Figure 9 shows an example of such a superconductor. We were successful in synthesizing 3 new superconductors with $T_c = 55$ K, 105 K and $T_c = 115$ K.^{14,15)}

3-2. Discovery of ladder lattice superconductors. A common characteristic of these superconductors is having a CuO_2 plane, which does not essentially introduce any new physics. Is it possible to discover yet more superconductors that belong to new categories? To search for such a situations, we focused on a ladder lattice, which has the structure shown in Fig. 10. The Takano Group of the Institute for Chemical Research at Kyoto University discovered SrCuO_2 with a two-leg ladder lattice, and Sr_2CuO_3 with a three-leg ladder lattice. It was experimentally demonstrated that two-leg ladder lattice substances had spin gaps and three-leg ladder lattice substances had no spin gaps.¹⁶⁾ Since then, T.M. Rice,¹⁷⁾ E. Dagotto¹⁸⁾ and others have pointed out the theoretical possibility of superconductivity in ladder lattice substances. They noted that superconductivity was expressed in the even-numbered ladder lattices and that spin gaps survived.

Are there really such convenient ladder lattice substances? It is amazing how well things work out in nature! Such a substance does exist in reality: $\text{Sr}_{14}\text{Cu}_{24}\text{O}_{41}$. It is called a ‘telephone-number’ compound due to its peculiar sequence of numbers: 14–24–41. As shown in Fig. 11, this substance’s crystal structure is layered with one-dimensional chain layers on a CuO_2 plane and two-leg ladder layers on a Cu_2O_3 plane. As is evident in its valence of $\text{Cu}^{2.25+}$, many holes already exist in this substance. These holes are mainly localized in one-dimensional chain layers, and their electrical conductivity is similar to that of semiconductors. What should be done to move these holes in the chain layers to ladder

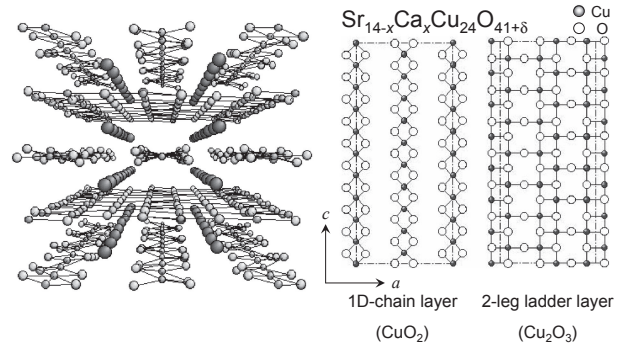


Fig. 11. Crystal structure of telephone number compound $\text{Sr}_{14}\text{Cu}_{24}\text{O}_{41}$, being composed of 1D-chain layer and 2-leg ladder layer.

layers? The easiest method is to shorten the distance between layers. To achieve this, the Sr site may simply be filled instead with Ca. In fact, when Sr is replaced by Ca in $\text{Sr}_{14-x}\text{Ca}_x\text{Cu}_{24}\text{O}_{41}$, its electrical resistivity decreases. In actual experiments, Ca may replace Sr only up to $x = 8.4$. Under a high oxygen pressure, however, Ca successfully replaced Sr up to $x = 13.6$. Unfortunately, however, superconductivity did not emerge. As a last resort, we measured its electrical resistivity under pressure in cooperation with Dr. Mori’s group in the Institute for Solid State Physics (ISSP) at the University of Tokyo, and in fact we found superconductivity of $T_c = 12$ K at 3 GPa (Fig. 12).¹⁹⁾ It was also confirmed by using the single crystal.²⁰⁾

4. Exploration of metal-based new superconductors

4-1. MgB_2 and its applications. During these explorations, we felt that we hit a dead-end with oxide superconductors, and decided to start exploring metal-based ones. Our guiding principle at that time was again the BCS theory. As shown in Eq. [1], T_c is proportional to the Debye temperature (Θ). In general, the lighter are the elements, the higher becomes the Debye temperature. It is expected that superconductivity with lighter elements would have a higher T_c . Thus, we focused on boron (B). I provided Jun Nagamatsu, an undergraduate student at that time, a research topic: to explore compounds of Mg with each of Ti and B. We included Ti because we thought that magnetic ions would play an essential role in some way, and B because it is a light element. Shortly after we began this study, Nagamatsu found a decrease in the magnetization, which was a precursory phenomenon of superconductivity. But

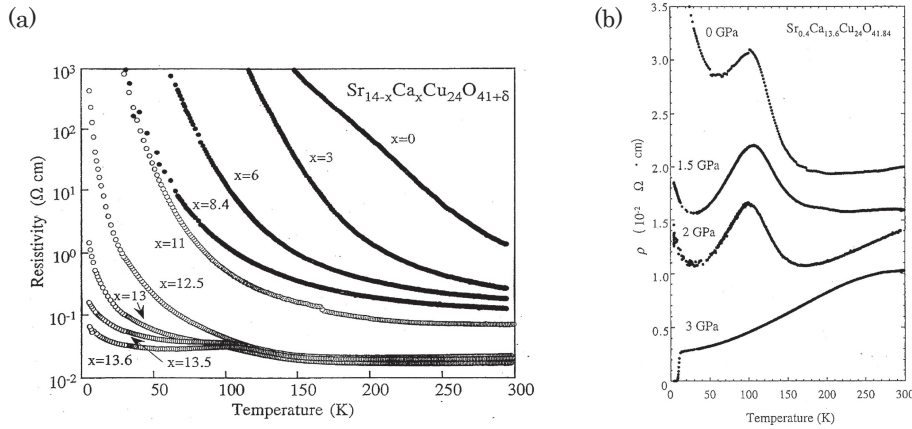
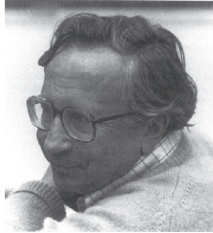


Fig. 12. (a) Temperature dependence of electrical resistivity in $\text{Sr}_{14-x}\text{Ca}_x\text{Cu}_{24}\text{O}_{41+\delta}$. With increasing x (Ca content), resistivity is decreased. (b) Pressure dependence of $\text{Sr}_{0.4}\text{Ca}_{13.6}\text{Cu}_{24}\text{O}_{41.84}$. Superconductivity appears at 3 GPa.¹⁹⁾

we had a hard time to make it a single phase. Finally, Nagamatsu was able to figure out that Ti was not necessary in this superconductivity, and the essential point was to create a substance with a very simple structure, called MgB_2 .²¹⁾ Figure 13 shows the electrical resistivity, and magnetic susceptibility, as a function of temperature. Figure 14 shows the crystal structure of MgB_2 . There were two points that surprised us upon the discovery of this substance. First, MgB_2 was a reagent available on the market. It was surprising that a substance commercially available as a reagent is actually a superconductor with a high T_c . This was picked up in the “News and Views” section of *Nature* with the title “Genie in a bottle” (pp. 23–24).²¹⁾ The second interesting news was that MgB_2 ’s crystal structure was called the AlB_2 structure, which consists of a honeycomb structure of B and a triangular grid of Mg, the layers of which created a characteristic 2-D lattice. In fact, this type of AlB_2 structure exists in large numbers (Table 2), and most of these substances were synthesized by B.T. Matthias. Strangely, however, Matthias did not synthesize MgB_2 . He would have regretted this oversight greatly if he were alive today. MgB_2 itself, obtains a high T_c through the electron-phonon interaction coupled with the strong lattice vibration of B, and it is believed that this is a typical (textbook) superconductivity, described by electron-phonon interaction. What is interesting about MgB_2 is that the band on the B plane (called σ band) and the band connecting the Boron and Mg ions (called the π band) both contribute to the superconductivity, which is called two-band superconductivity. Figure 15 shows this band structure and the Fermi surface.²²⁾

Table 2. List of the MB_2 -series materials synthesized by B.T. Matthias, except for the MgB_2

	BeB_2	
	MgB_2	AlB_2
	ScB_2	TiB_2
	YB_2	ZrB_2
	BaB_2	HfB_2



Bernd Matthias
Bernd Theodor Matthias

	VB_2	CrB_2	MnB_2						
	NbB_2	MoB_2	TcB_2	RuB_2					
	TaB_2	WB_2	ReB_2	OsB_2					

LuB_2	CrB_2 $T_c = 86$ K (J.Castaing <i>et al.</i> <i>J.Phys.Chem.Solids</i> (1972) Vol.33 533)
UB_2	MnB_2 $T_c = 143$ K (L.Andersson <i>et al.</i> <i>Solid State Communications</i> Vol.4 77 (1966))
PuB_2	$\text{TiB}_2, \text{VB}_2, \text{CrB}_2, \text{MnB}_2, \text{ZrB}_2, \text{MoB}_2, \text{HfB}_2, \text{TaB}_2$ $T_c = 0.42$ K
	NbB_2 $T_c = 0.62$ K (L.Leyarovska <i>et al.</i> <i>J.Less-common Metals</i> 67 (1979) 249)

Thus, MgB_2 is a typical BCS-type superconductor, mostly explained by the electron-phonon interaction, but its most interesting point is its applications. The critical temperature (T_c) is not the only parameter to be considered in applications. In general, superconductivity breaks down in a strong enough magnetic field, termed the critical magnetic field (H_c). Superconductivity also breaks if a large amount of electric current is applied, termed the critical current (J_c). In short, superconductivity exists in a region defined by a critical temperature, critical magnetic field and critical current. For the widest range of practical applications, superconductors with high T_c , H_c , J_c are needed. Unlike T_c , H_c and J_c may be increased by various means. For

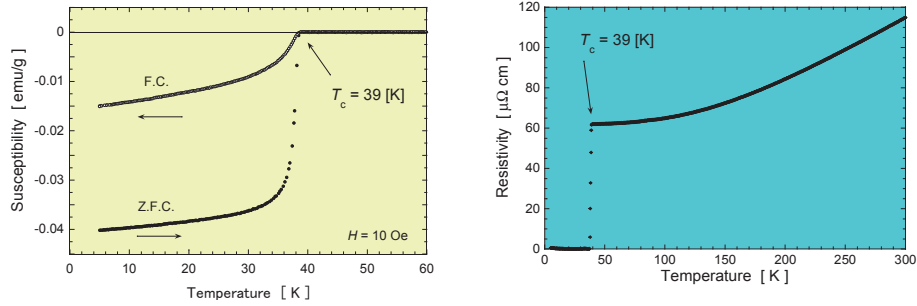


Fig. 13. Electrical resistivity and magnetic susceptibility of MgB_2 as a function of the temperature.²¹⁾

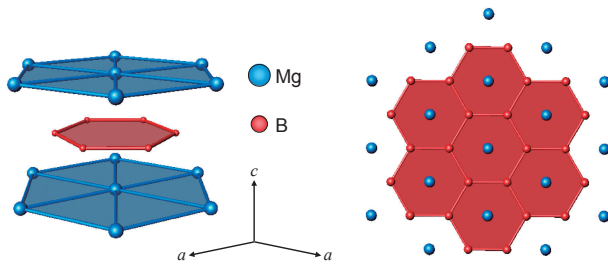


Fig. 14. Crystal structure of MgB_2 .²¹⁾

example, J_c and H_c is drastically increased by mixing in small amounts of impurities.

To be used in superconducting magnets and transmission cables, MgB_2 must be turned into wires. In that regard, MgB_2 's advantages include:

- (1) It may be used at a relatively high temperature (approximately 20 K), which is impossible for

conventional metal-based superconducting materials.

- (2) Since bonding between crystal grains is strong, which makes it possible to transfer a large amount of superconducting current from one crystal grain to an adjacent one, it is not necessary to align the direction of crystal grains (as in copper oxide high-temperature superconductors). Therefore, it is relatively easy to create wires.

- (3) From the perspective of resources, both Mg and B are abundant raw materials that can be obtained at relatively low prices in a stable supply.

Values of H_c and J_c for MgB_2 may be enhanced with the processing procedures mentioned above. Thus, many studies have been conducted globally to create wires since the discovery of MgB_2 superconductivity, and wires longer than several km have been produced experimentally.

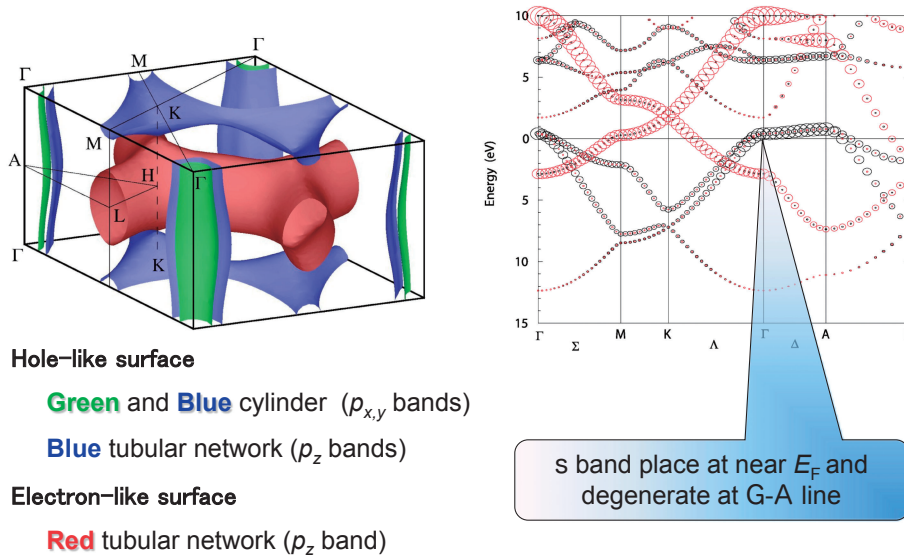


Fig. 15. The band structure and the Fermi surface of MgB_2 .²²⁾

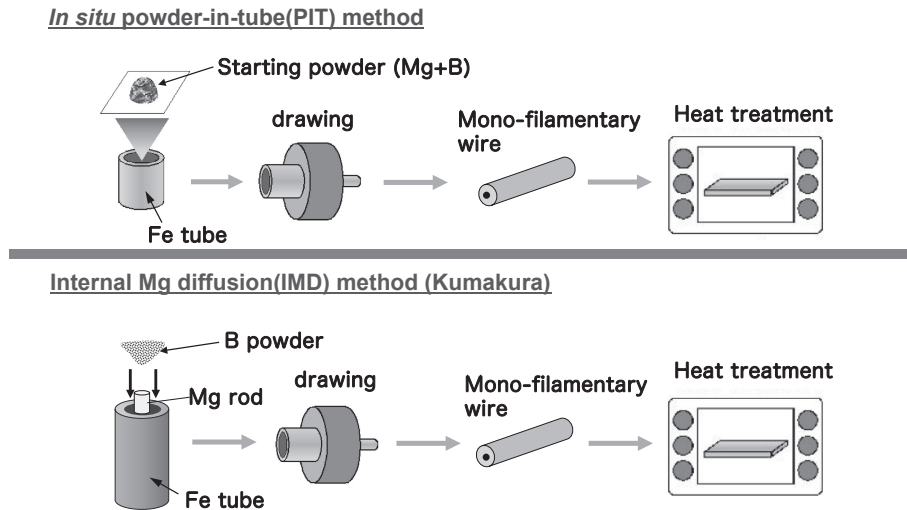


Fig. 16. Two fabrication methods to make a MgB_2 wire. 1) *In situ* powder-in-tube (PIT) method. 2) Internal Mg diffusion (IMD) method.²³⁾

Some of the methods for the creation of MgB_2 wires have been proposed based on past knowhow.²³⁾ Figure 16 shows two fabrication methods: ① *In situ* Powder-in-tube (PIT) method and ② Internal Mg diffusion (IMD) method. Recently, the most common method has been Powder-in-Tube (PIT), where a starting powder is stuffed into metal tubes, and processed before and/or after placement in the tube. There are basically two PIT methods. One is an *ex-situ* method, where pre-processed MgB_2 powder is stuffed into metal tubes, such as stainless steel. The other is an *in-situ* method, where a mixed powder of Mg and B is stuffed in a tube to fabricate tapes, which are then heat-treated. In the *ex-situ* method, the greatest advantage is that a worthwhile J_c may be obtained, even without the heat-treatment process. A further heat treatment (annealing) improves the binding between crystal grains, leading to a higher J_c . In the “*in-situ*” method, the reactivities of Mg and B are enhanced with a heat treatment, and at the same time, unlike in the *ex-situ* method, there is our advantage that the crystal grains are rarely oriented.

Another effective method to increase the MgB_2 core density is an internal Mg diffusion (IMD) process.²⁴⁾ The IMD method is believed to provide a higher J_c due to our improved connectivity of MgB_2 . The starting materials used are also important. Recently, there have been many reports that the characteristics of J_c are improved when a trace amount of minute impurities is added to a mixed powder of Mg and B. Currently, the most effective method is to add minute SiC particles that are in the

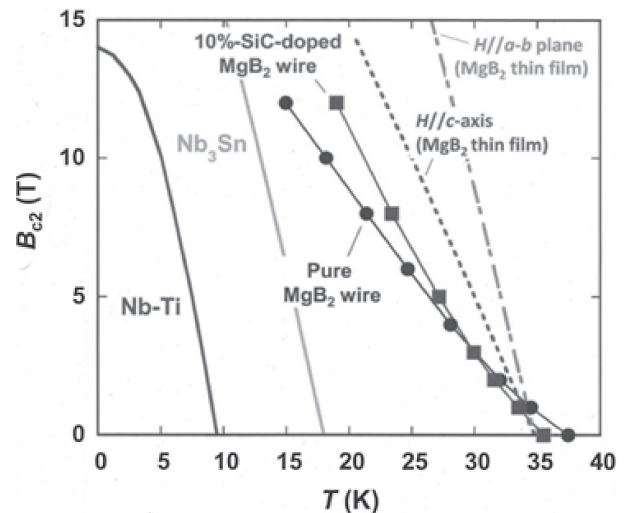


Fig. 17. Temperature dependence of B_{c2} in MgB_2 wires.²³⁾

nanometer range. Figure 17 shows the temperature dependence of B_{c2} in MgB_2 tapes with no additives, and those with SiC added. In wires with SiC added, B_{c2} for 4.2 K was as high as 30 T. This value is equal to or greater than the value of B_{c2} in Nb_3Sn wires. The B_{c2} in 20 K wires ranges up to 11 T. This shows that currently used utility wires may be replaced with MgB_2 .

Naturally, for use in magnet wires, the magnetic field dependence of J_c is an important factor. Figure 18 shows the present status of MgB_2 wires prepared by both the PIT and IMD methods. As shown in Fig. 18, for the practical level at 20 K and

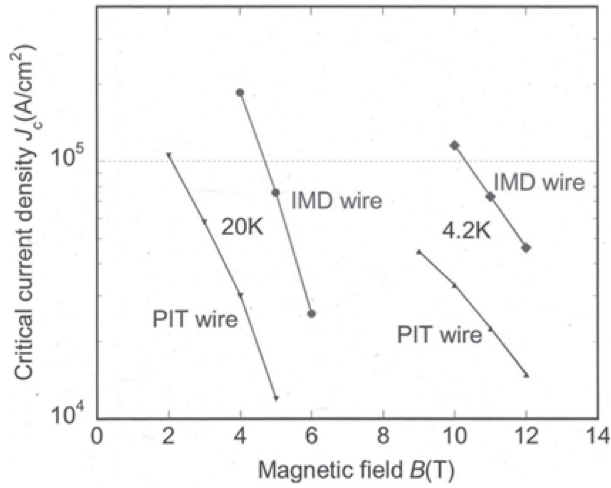


Fig. 18. Present status of critical current density J_c (A/cm^2) vs. magnetic field B (T).²³⁾

2 T, J_c in PIT wire keeps $J_c \sim 10^5 \text{ A}/\text{cm}^2$. Unfortunately, J_c reduces to $1.2 \times 10^4 \text{ A}/\text{cm}^2$ at 20 K and 5 T. However, there has recently been rapid progress in this area. By using the IMD method, it reached to almost $9 \times 10^4 \text{ A}/\text{cm}^2$ at 20 K and 5 T. The future is promising.

4-2. Y_2C_3 . Since discovering the MgB_2 superconductor, we have conducted broad explorations of superconductors that include light elements, such as boron (B) and carbon (C). As a result, we found that Y_2C_3 is a superconductor ($T_c = 18 \text{ K}$) synthesized under high pressure. Figure 19 shows the temperature dependence of the resistivity and the susceptibility at ambient pressure. T_c is controllable by a

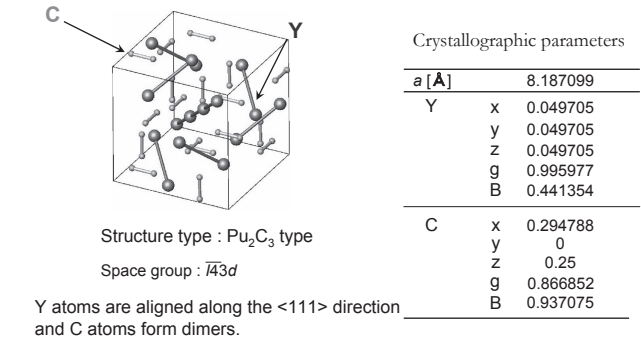
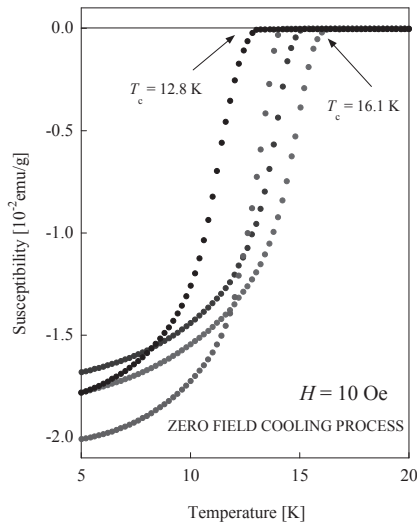


Fig. 20. Crystal structure of Y_2C_3 to be the Pu_2C_3 -type with (b.c.c.) structure.

synthesis condition.^{25)–27)} Afterwards, we found that this substance had already been reported by Krupka *et al.*²⁸⁾ as having a maximum T_c of 11.5 K. Figure 20 shows its crystal structure to be the Pu_2C_3 -type, with a body-centered cubic structure (b.c.c.). Its Y atoms line up along the $\langle 111 \rangle$ direction, and its carbon atoms form dimers, with an extremely short C-C bond length. It is expected that its C-C stretching phonon mode is very high. Therefore, the relatively high T_c of Y_2C_3 is thought to be the result of electron-phonon coupling between high-frequency phonons and the C-C antibonding state in the vicinity of the Fermi level. A characteristic of both Y_2C_3 and La_2C_3 , which has the same structure as Y_2C_3 , is that they are superconductors with two gaps. This was first suggested by NMR measurement of spin-lattice relaxation.²⁹⁾ It was then clarified further in a μSR measurement.³⁰⁾ Figure 21 shows the temperature

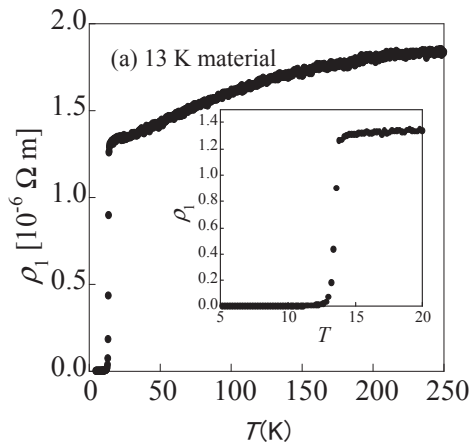


Fig. 19. Temperature dependence of resistivity and susceptibilities in Y_2C_3 .^{25),27)}

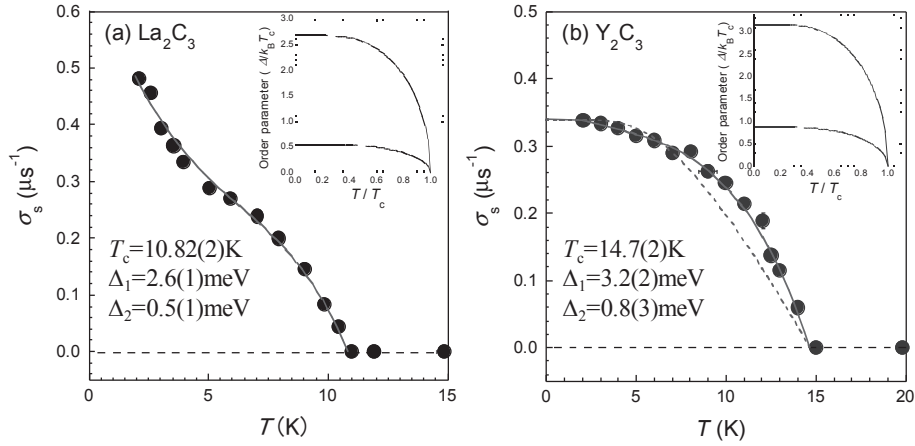


Fig. 21. Temperature dependence of the muon spin relaxation rates of La_2C_3 and Y_2C_3 . Solid and dashed lines are fitted with the s-wave's phenomenological double-gap model.³⁰⁾

dependence of the muon spin relaxation rates of La_2C_3 and Y_2C_3 . Solid and dashed lines are fitted with the s-wave's phenomenological double-gap model.³⁰⁾ It was theoretically suggested that in the crystal structure of Y_2C_3 , a strong spin-orbit interaction might lead to a mixed state of symmetric isotropic and anisotropic superconducting properties due to the lack of a space inversion symmetry. It was reported later that B_{c2} is very high, at approximately 30 Tesla, which may be related to the above state.

4-3. Superconductivity of carrier-doped semiconductors.

(1) *Superconductivities of boron-doped diamond and Si.* Diamonds, famously known as jewels, do not allow the flow of electricity, as is evident from their sparking. Surprisingly, however, it was discovered that diamonds become superconductive if carrier-doped ($T_c = 3\text{ K}$).³¹⁾ By making films even thinner, its T_c was raised to 12 K.³²⁾ The superconducting transition $T_c = 0.35\text{ K}$ was also reported when B was doped into silicon (Si), with a similar crystal structure.³³⁾ Both substances are typical wide-gap semiconductors with the well-known diamond structure. If highly concentrated hole carriers are doped to those wide-gap semiconductors, superconductivity will be created. Since then, many theoretical studies have been actively conducted, indicating the possibility of the emergence of superconductivity at considerably higher temperatures, depending on the doped B atoms' order or alignment.³⁴⁾

We tried to create superconductivity by B replacement (hole doping) in SiC, with characteristics similar to those of diamonds and Si, and discovered that its bulk was a superconductor with $T_c = 1.4\text{ K}$.³⁵⁾

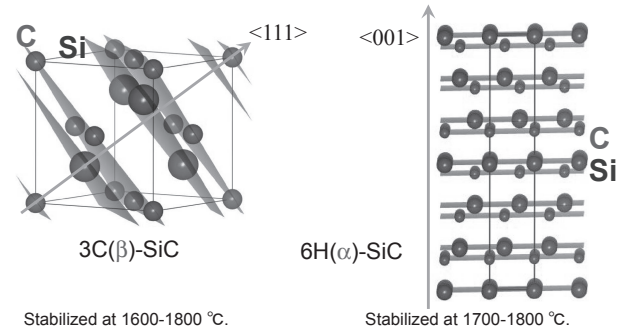


Fig. 22. Crystal structure of the 3C-SiC and 6H-SiC, respectively.

We also tried to use aluminum (Al) as a hole dopant in the same manner, and verified a superconducting transition at a similar T_c ($\approx 1.4\text{ K}$).³⁶⁾ In the following sections, the basic physical properties that have been discovered so far are explained.

(2) *Crystal structure of SiC.* SiC has a crystal structure in which C and Si are basically placed at even intervals in a diamond-type structure. However, when one looks precisely, many different structures emerge (polytype: crystal polymorphism), depending on the type of lamination layer formed. Although 200 or more polytypes have been verified currently, 3C-, 4H-, 6H-, and 15R-SiC (Ramsdell notation system) are the most important in applications, and have a high probability. In this notation system, the first number refers to the number of Si-C unit layers included in the layer direction (c, axis direction) during one cycle; C, H and R are the initial letters of crystal systems (C: cubic, H: hexagonal, R: rhombo-

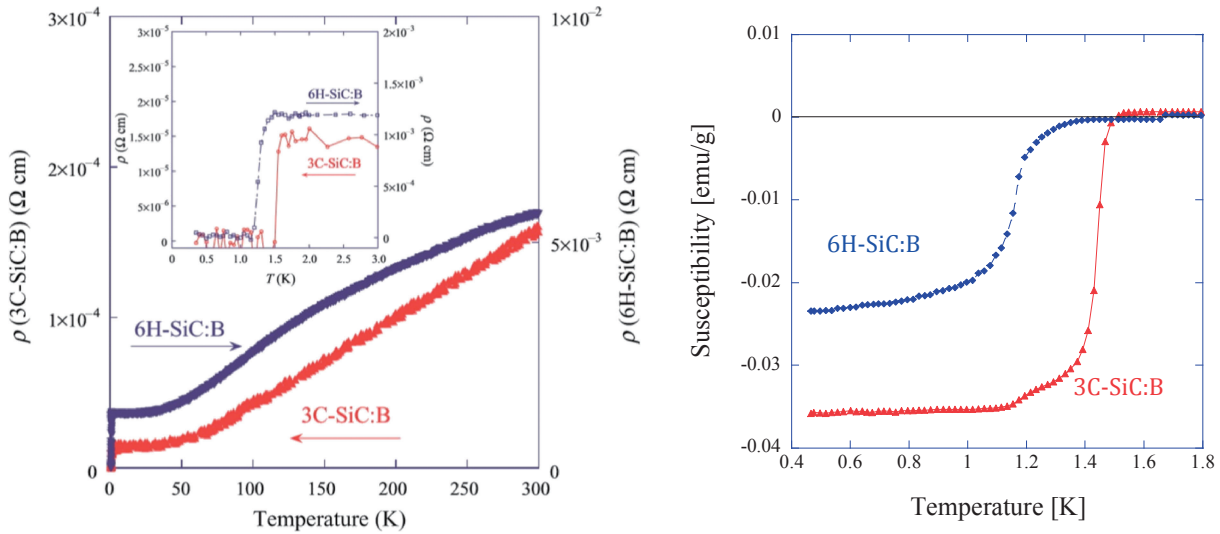


Fig. 23. Temperature dependences of the electrical resistivities and magnetic susceptibilities.³⁶⁾

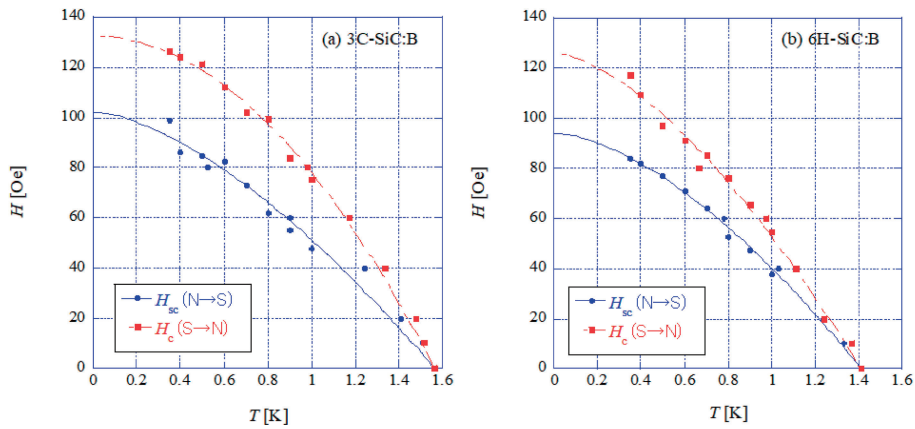


Fig. 24. H - T phase diagram for (a) B-doped 3C-SiC(3C-SiC:B) and (b) B-doped 6H-SiC(6H-SiC:B), determined from the onset of superconductivity during a T -scan and H -scan of resistivity.

hedral). The zincblende structure that often emerges in other semiconductors is expressed as 3C, and the wurtzite structure is 2H. All band structures are of the indirect transition type, the same as that of Si. Among these polytypes, we focused on 3C-SiC and 6H-SiC (Fig. 22), and attempted hole doping in each of them.

(3) *Superconductivity of B-doped SiC.* Figure 23 shows the temperature dependence of the electrical resistivity in SiC samples (3C-SiC:B, 6H-SiC:B), where B was doped into 3C-SiC and 6H-SiC. In both, though the T_c values are low (approximately 1.4 K), a sharp superconducting transition can be observed. Also, in these transitions, substantial Meissner diamagnetism has been observed in measurements of the DC magnetic susceptibility (Fig. 23),

and specific-heat jumps have been observed, confirming bulk superconductivity. It is considered that differences in T_c and the residual resistance between these substances show their disparity in reactivity, since 3C-SiC is in its low-temperature stabilized phase and 6H-SiC is in its high-temperature stabilized phase.

Figure 24 shows a magnetic field *vs.* temperature phase diagram of the superconducting state, as determined by measuring the electrical resistivity with changing temperature under a constant magnetic field (T -scan), and also with a changing magnetic field under a constant temperature (H -scan). As shown in Fig. 24, T_c during the cooling process starting from $T > T_c$ and the T_c observed during the warming process do not match. This

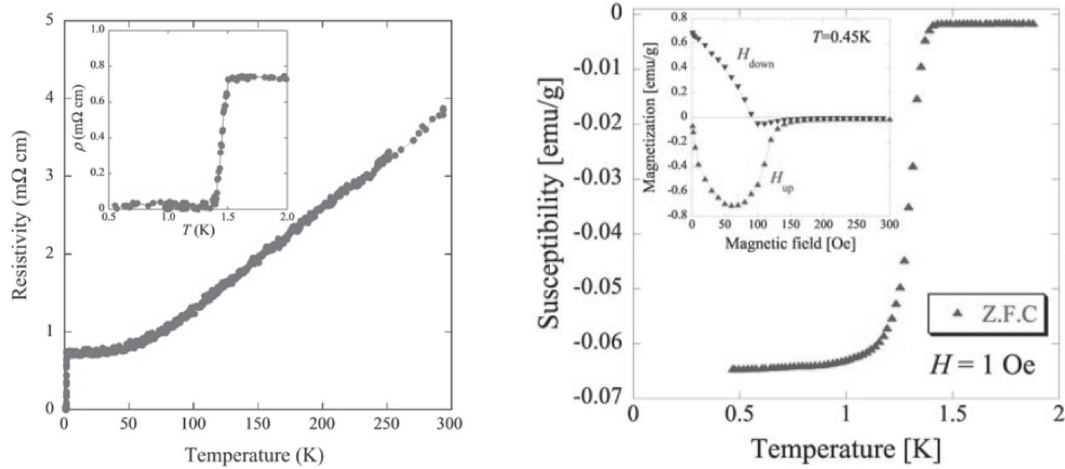


Fig. 25. Temperature dependences of the electrical resistivity and magnetic susceptibility in SiC(3C-SiC:Al), where 3C-SiC was doped with Al.³⁶⁾

strongly suggests that B-doped SiC is a Type I superconductor. In general, simple elements, such as tin (Sn) and lead (Pb), become Type I superconductor, and Type I superconductivity in a chemical compound is very rare. The above-mentioned B-doped diamonds and B-doped Si are reported to be Type II superconductors.

(4) *Superconductivity of Al-doped SiC.* Figure 25 shows the temperature *vs.* electrical resistivity and magnetic susceptibility in SiC samples (3C-SiC:Al), where 3C-SiC was doped with Al. T_c was approximately 1.5 K, almost equal to that of the above B-doped SiC, for which superconductivity can be verified. Also, in this transition, substantial Meissner diamagnetism has also been observed in measurements of the DC magnetic susceptibility, and a specific-heat jump has also been observed, confirming bulk superconductivity.

Figure 26 shows a magnetic field and temperature phase diagram of the superconducting state, as determined by measuring the electrical resistivity with changing the temperature under a constant magnetic field, and also with changing magnetic field under a constant temperature. Unlike the above B-doped SiC, under a finite magnetic field, that observed during the cooling process matched the T_c observed during the warming process, suggesting that this is a Type II superconductor, the same as B-doped diamond and B-doped Si.

(5) *Discussion and outlook.* The superconductivity of B-doped SiC involves almost the same carrier density as the superconductivity in B-doped diamond and B-doped Si, and its crystal structure is almost the same as that of diamond. It is very

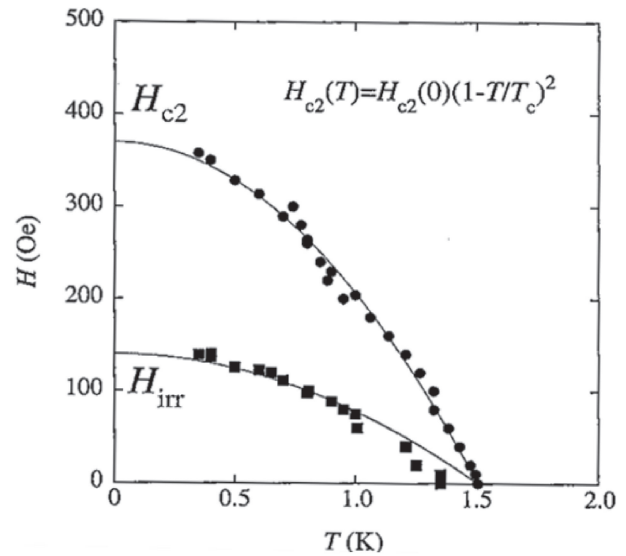


Fig. 26. Temperature dependence of the upper critical field H_{c2} and the irreversibility field H_{irr} in 3C-SiC:Al.³⁶⁾

interesting to understand why only B-doped SiC is a Type I superconductor. Our experimental results may contribute to a qualitative understanding of this question by using the impurity level formed in semiconductors.

Table 3 summarizes the normal-state properties, including the impurity levels (E_A), and also the superconducting parameters of B-doped diamond (C:B), B-doped Si (Si:B), B-doped SiC (SiC:B), and Al-doped SiC (SiC:Al).

Although B-doped Si has been reported as forming Type II superconductors, recent studies

Table 3. Superconducting and normal state properties for SiC:Al, SiC:B, diamond (C):B and Si:B³⁶⁾

	SiC:Al	SiC:B	C:B	Si:B
n (cm ⁻³)	7.06×10^{20}	1.91×10^{21}	1.80×10^{21}	2.80×10^{21}
γ_n (mJ/molK ²)	0.35	0.294	0.113	—
ρ_0 (mΩcm)	0.746	0.06	2.5	0.13
RRR	5.3	10.0	0.9	1.2
T_c (onset) (K)	1.5	1.45	4.50	0.35
$H_c(0)$ (Oe)	—	115	—	—
$H_{sc}(0)$ (Oe)	—	80	—	—
$H_{c2}(0)$ (Oe)	432	—	4.2×10^4	4000
k_F (nm ⁻¹)	2.8	3.8	3.8	—
m^* (m_{el})	2.0	1.2	1.7	—
v_F (m/s)	1.6×10^5	3.8×10^5	—	—
l (nm)	2.2	14	0.34	—
$\xi(0)$ (nm)	87	360	80(9)	(20)
$\lambda(0)$ (nm)	281	130	160	—
κ_{GL}	3.2	0.35	2(18)	—
E_A (eV)	~ 0.25	~ 0.29	0.37	0.045

suggest that they may be Type I superconductors, as revealed by samples with improved quality. B-doped Si's Type I superconductivity may have been hidden due to the crystals' irregularities and/or disorder, resulting in their being reported as Type II superconductivity despite the fact that it is essentially Type I superconductivity. What is observed from these parameters is that the disorder of the impurity or its level has a large impact if the acceptor level is deep, and leads to Type II superconductivity. SiC:Al may be positioned on the border of Type I and Type II superconductivities in hole-doped superconductors. Also, since the state density in the vicinity of SiC's Fermi level is mainly due to the Si structure, it is inferred that the Si may be more important than the C for superconductivity. Based on structural analysis results, it is considered that Al may show Type II superconductivity due to the stronger impact of any disorder of Al, since it is supposed that B is then transposed to the C site and Al is transposed to the Si site.

4-4. New superconductor with a cage-type structure— $R_5T_6Sn_{18}$ (R = Sc, Y, Lu; T = Rh, Ir). In this section, a new superconductor with a cage-type structure that we have worked on is briefly explained. $R_5T_6Sn_{18}$ (R = Sc, Y, Lu; T = Rh, Ir) was first discovered by Remeika *et al.*³⁷⁾ We, however, discovered a totally new experimental fact by systematically synthesizing single-crystal samples of it.³⁸⁾ $R_5T_6Sn_{18}$ has a cage-type structure consisting

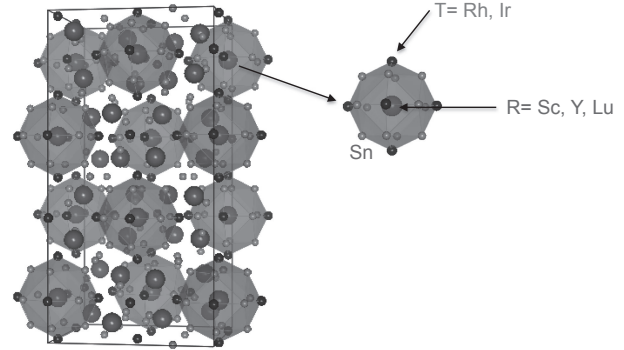


Fig. 27. Cage-type crystal structure of $R_5T_6Sn_{18}$ (R = Sc, Y, Lu; T = Rh, Ir).³⁸⁾

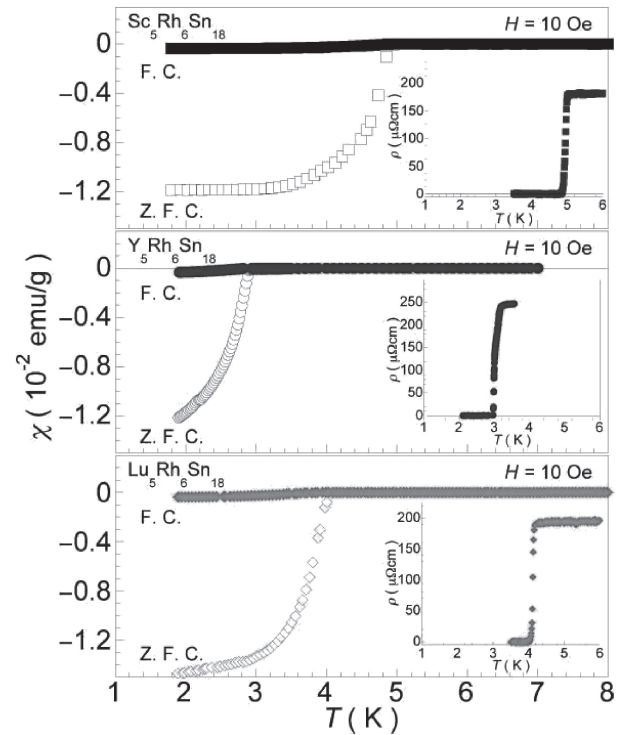
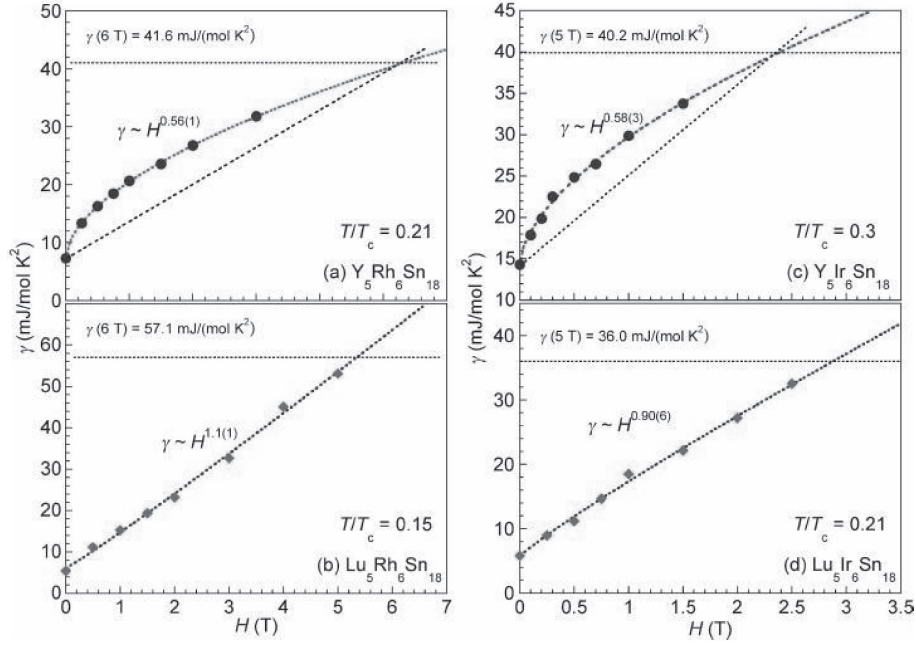


Fig. 28. Temperature dependence of the magnetic susceptibility in $R_5Rh_6Sn_{18}$ (R: Sc, Y and Lu).³⁸⁾

of $R_5T_6Sn_{18}$ (Fig. 27). This is a group in which the superconducting state changes as the R element included in the cage changes. The superconducting transition temperatures are $T_c = 5, 3,$ or 4 K, for R = Sc, Y, or Lu, respectively. Sc, with the smallest ionic radius, has the highest T_c (Fig. 28). The most noteworthy characteristic of this group is that the superconducting gaps change substantially depending on the rare-earth ion, R.³⁸⁾ The magnetic field dependencies of the quasiparticle state densities

Fig. 29. Quasiparticle state density (γ) vs. magnetic field.³⁸⁾Table 4. Superconducting parameters obtained from experiments in $R_5T_6Sn_{18}$ (R: Sc, Y, Lu, T: Rh, Ir). It is noted that anisotropic superconductors only appear for R = Y³⁸⁾

Space group	Sc ₅ Rh ₆ Sn ₁₈	Sc ₅ Ir ₆ Sn ₁₈	Y ₅ Rh ₆ Sn ₁₈	Y ₅ Ir ₆ Sn ₁₈	Lu ₅ Rh ₆ Sn ₁₈	Lu ₅ Ir ₆ Sn ₁₈
	I_{41}/acd	I_{41}/acd	I_{41}/acd	$Fm\bar{3}m$	I_{41}/acd	I_{41}/acd
Gap asymmetry	isotropic	isotropic	anisotropic	anisotropic	isotropic	isotropic
a (nm)	1.3601	1.3595	1.3792	1.3735	1.3671	1.3602
c (nm)	2.7198	2.7180	2.7498	—	2.7330	2.7315
T_c (K)	5.0	1.0	3.0	2.1	4.0	3.0
$\mu_0 H_c(0)$ (mT)	99.1(1)	12.2(1)	50.1(4)	30.4(1)	75.0(2)	47.6(1)
$\mu_0 H_{c1}(0)$ (mT)	5.64(1)	—	2.49(2)	1.46(1)	4.38(1)	1.87(2)
$\mu_0 H_{c2}(0)$ (T)	7.24(5)	—	4.21(6)	2.91(6)	5.58(5)	3.90(10)
$\lambda(0)$ (nm)	34.2(1)	—	51.4(2)	67.2(1)	38.8(1)	59.2(2)
$\xi(0)$ (nm)	6.74(1)	—	8.84(4)	15.9(1)	7.68(2)	13.0(1)
$\kappa(0)$	51.7(1)	—	59.1(4)	62.1(1)	50.5(1)	66.8(1)
γ (mJ/(mol·K ²))	51.0(4)	27.3(4)	37.8(4)	32.1(2)	49.1(4)	31.9(1)
Θ_D (K)	276(2)	246(2)	185(1)	212(2)	158(1)	193
$\Delta(0)$ (meV)	0.990(3)	0.140(1)	—	—	0.719(2)	0.544(3)
$\Delta C_e/\gamma_n T_c$	2.55(36)	1.39	1.96	1.68	2.02	1.83
$2\Delta(0)/k_B T_c$	4.26(3)	3.26(6)	—	—	4.12(2)	4.07(5)

(γ) resulting from specific-heat measurements in Lu₅Ir₆Sn₁₈ and Lu₅Rh₆Sn₁₈ at various temperatures are $\gamma \sim H^{0.90}$ and $\gamma \sim H^{1.1}$, respectively, representing isotropic superconducting gaps.³⁸⁾ While these isotropic superconducting gaps may be explained by the BCS theory,³⁹⁾ the magnetic-field dependencies of γ in Y₅Ir₆Sn₁₈ and Y₅Rh₆Sn₁₈ are $\gamma \sim H^{0.58}$ and

$\gamma \sim H^{0.56}$, respectively, representing anisotropic superconducting gaps^{38),39)} (Fig. 29).

Table 4 summarizes the normal and superconducting parameters. Unfortunately, the physical reason why such a major physical property changes so substantially when rare-earth elements are changed is not yet clear.

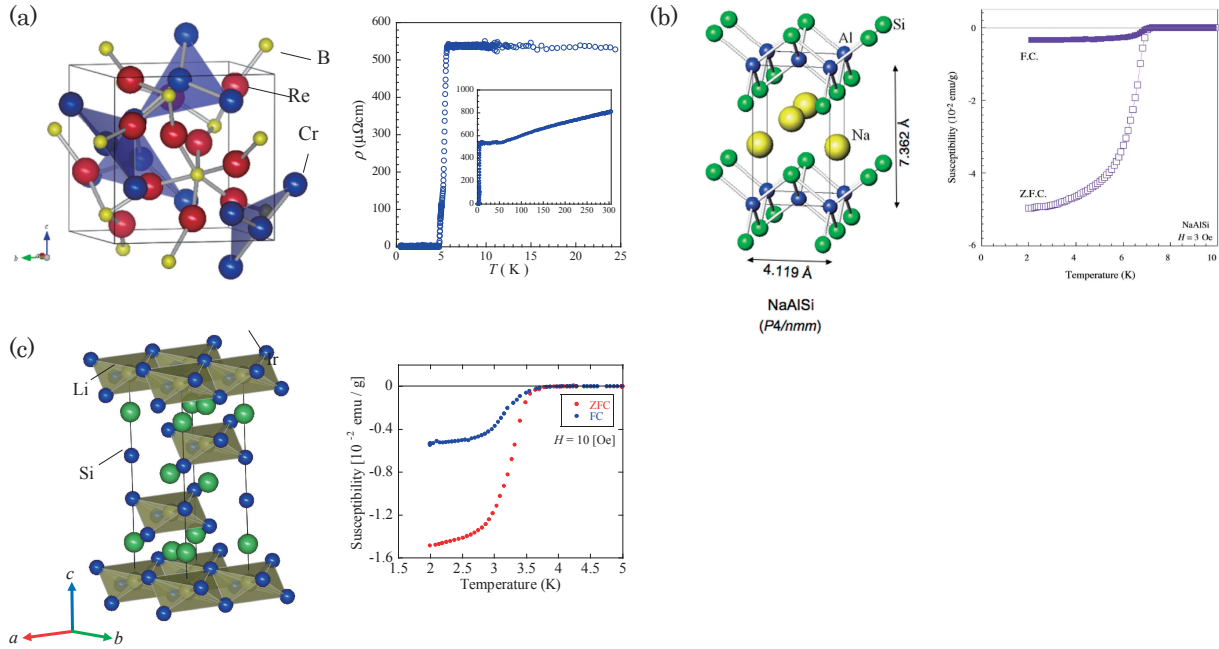


Fig. 30. Typical examples of superconductivities and crystal structures chosen from Table 5. (a) $\text{Cr}_2\text{Re}_3\text{B}$,⁶¹⁾ (b) NaAlSi ,⁶²⁾ and (c) Li_xIrS_2 .

5. Summary and outlook

5-1. Summary—Discovery of new superconductors— In the previous sections, the main topics concerning the new superconductors discovered in our laboratory are described, which can be categorized into two groups:

1. Cu-oxide superconductors.
 - 1-1 Cu-oxide system having CuO_2 planes.
 - 1-2 Ladder lattice superconductor.
2. Exploration of metal based new superconductors.
 - 2-1 MgB_2 and its application.
 - 2-2 Y_2C_3 .
 - 2-3 Carrier-doped wide-gap semiconductors.
 - 2-4 New superconductor with a cage-type structure: $\text{R}_5\text{T}_6\text{Sn}_{18}$ ($\text{R} = \text{Sc}, \text{Y}, \text{Lu}$; $\text{T} = \text{Rh}, \text{Ir}$).

These superconductors are representative materials that we discovered.

Finally, we summarize here all of the superconductors discovered in our laboratory (Table 5).

From the Table 5, we chose typical examples of superconductivities as well as crystal structures in $\text{Cr}_2\text{Re}_3\text{B}$,⁶¹⁾ NaAlSi ,⁶²⁾ and Li_xIrS_2 (Fig. 30).

5-2. Outlook for the higher- T_c superconductors. In a previous section, we described what we have done. Next is our future prospects concerning what we should attack. We present here several

candidates to achieve higher- T_c ($T_c \geq 100$ K) superconductors.

(1) *Hydride system.* The first one is the hydride system. Hydride system has long been expected to be a candidate of room-temperature superconductor. Unfortunately, however, only a moderate $T_c \sim 17$ K was observed in the Pd hydrate experimentally. Recently, much attention has been paid to superconductivity at 203 K at ultra-high pressure in SH_3 .⁶³⁾ Subsequently, superconductivity above 260 K (near room temperature!) has been discovered in LaH_{10} .^{64,65)} Disappointedly, it has only been achieved under ultra-high pressure at around 200 GPa, which is not a practical pressure. The next step is to discover a new hydride system, and to realize a high- T_c superconductor under ambient pressure.

(2) *Superconductivity in 4d, 5d system.* The second big problem is that “Is there any other existing transition metal (except for Cu, Fe) oxide/chalcogenide superconductor? In particular, a high- T_c superconductor of the 4d, 5d system is unexplored?”. This will be discussed in the next section.

(3) *High- T_c superconductor originated from charge fluctuation or valence skipping system.* It is well known that the origin of a high- T_c superconductor in Cu-oxide is due to magnetic fluctuation instead of some electron-phonon interaction. In this sense, the

Table 5. New superconductors discovered in the Akimitsu laboratory

Cu-oxide based new superconductors

Year	Superconductor	T_c (K)	Reference
1987	Bi-Sr-Cu-O	6	5), 6)
1988	Nd-Ce-Sr-Cu-O	28	8), 9)
1989	(Eu,Ce)-(Ba,Ln)-Cu-O (Ln = Nd, Sm, Eu)	43	40)
1992	(Y,Ca)-Sr-Cu(CO ₃)-O	63	41)
1992	(Bi,Pb)-Sr-Cu-(CO ₃)-O	41, 54	42)
1993	Sr-Ca-Cu-(CO ₃)-(BO ₃)-O	33, 55, 105, 115	14), 15)
1993	Tl-(Ba,Sr)-Cu-(CO ₃)-O	70	43)
1993	Hg-Ba-Sr-Cu-(CO ₃)-O	66	44)
1994	Ba-Ca-Cu-(CO ₃)-(BO ₃)-O	120	45)
1994	(Ca,Na)-Ca-Cu-O-Cl	49	46)
1995	(Ca,A)-Cu-O-Br (A = Na, K)	19	47)
1996	Ba-Ca-Cu-O-F	38, 106, 108	
1996	Sr-Ca-Cu-O(14-24-41)	12	19)
1998	Cu-Sr-(Y,Ce)-Cu-O	43	48)
1999	Ru-Sr-Y-Cu-O	40	49)

Metal-based new superconductors

Year	Superconductor	T_c (K)	Reference
1984	(Nb,Ta)Se ₃	4	1)
2001	MgB₂	39	21)
2003	Re-B	5	50)
2004	Y ₂ C ₃	18	25)
2006	(W,Mo)-Re-(B,C)	7, 8	51)
2007	NaAlSi	7	62)
2007	SiC:B	1.4	35)
2008	SiC:Al	1.5	36)
2008	AlN _x	2.8	
2009	W ₅ Si ₃	2.8	52)
2010	YSn ₃	7	53)
2010	Y ₃ Pt ₄ Ge ₆	2.6	54)
2011	W ₅ SiB ₂	5.8	55)
2012	(Ta,W) ₅ SiB ₂	6.5	56)
2012	KAlX (X = Si, Ge)	3.5, 4	
2012	AE(TM,Si) ₂ (AE = Ca, Sr, Ba; TM = Ni, Pd, Pt, Cu, Ag, Au)	0.9–3.5	57)
2013	KSn ₂	3.2	58)
2013	As(Al,Ge) ₄₆	4, 4.4	59)
2013	Lu ₂ SnC	5	60)
2014	Cr ₂ Re ₃ B	6	61)

charge fluctuation is another candidate to produce high- T_c superconductivity, for example Ba_{1-x}K_xBiO₃ ($T_c \sim 30$ K) is believed to be a charge fluctuation-mediated superconductor.

However, why can we not get a higher- T_c ($T_c \geq 100$ K) superconductor mediated by charge fluctuation? This is a third big problem.

5-3. Our present work. In this section, we briefly describe what we are presently working on.

Recently, much attention has been paid to superconductivity in the Iridate system. If superconductivity is realized in this system with the strong spin-orbit coupling (S.O.C), it will open the new dimension in condensed-matter physics. In partic-

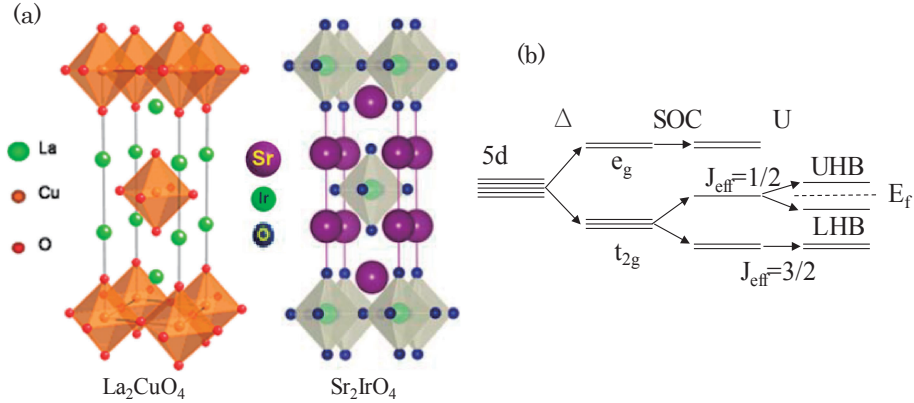


Fig. 31. (a) Crystal structure of La_2CuO_4 and Sr_2IrO_4 . (b) Schematic diagram of the $5d$ energy levels split by the crystal field (Δ), spin-orbit coupling (SOC), and on-site Coulomb repulsion (U) leading to the formation of unoccupied (upper) and occupied (lower) Hubbard bands at around the Fermi level from the $J_{\text{eff}} = 1/2$ band and the fully occupied $J_{\text{eff}} = 3/2$ band.

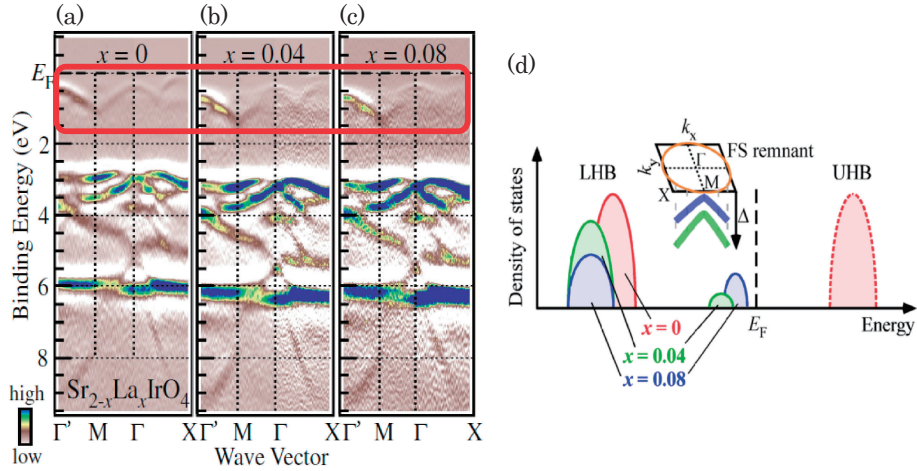


Fig. 32. (a)–(c) Second derivative of ARPES intensity plots as a function of the binding energy and wave vector on $\text{Sr}_{2-x}\text{La}_x\text{IrO}_4$ ($x = 0, 0.04$ and 0.08) measured along the k direction. (d) Schematic graph of the doping-induced change in the electronic structure of $\text{Sr}_{2-x}\text{La}_x\text{IrO}_4$ derived from our ARPES study.⁶⁹⁾

ular, $\text{Sr}_2\text{IrO}_4/\text{Ba}_2\text{IrO}_4$ has been predicted to be a high-temperature superconductor upon electron doping,⁶⁶⁾ since it highly resembles the cuprate in the crystal structure and magnetic coupling constant. Particularly, the remarkable resemblance between $\text{Sr}_2\text{IrO}_4/\text{Ba}_2\text{IrO}_4$ and La_2CuO_4 makes a good candidate to expect unconventional HTSC in $\text{Sr}_2\text{IrO}_4/\text{Ba}_2\text{IrO}_4$ (Fig. 31). Indeed:

- 1) A low-temperature STM study⁶⁷⁾ on the K-doping (effectively electron doping) in the clean surface of Sr_2IrO_4 demonstrates the clear spin gap state.
- 2) Moreover, Y.K. Kim *et al.* observed the low-temperature nodal Fermi surface and high-temperature Fermi arcs.⁶⁸⁾

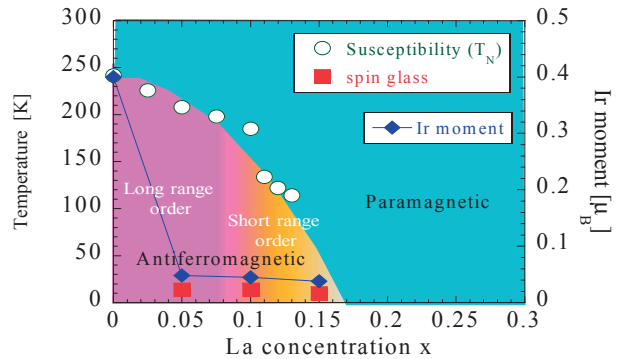


Fig. 33. Magnetic phase diagram of $\text{Sr}_{2-x}\text{La}_x\text{IrO}_4$ determined from magnetic susceptibility and μSR measurements.⁷⁰⁾

These experimental results suggest clear evidence of a d-wave pairing correlation. However, direct evidence of superconductivity, such as zero resistivity ($E = 0$) and the Meissner effect ($\mathbf{B} = 0$), can not be observed in the bulk system. We have tried to observe evidence of superconductivity in a carrier-doped bulk material. Recently, we published our present experimental data concerning this problem in the papers.^{69)–71)}

In particular, Terashima *et al.*⁶⁹⁾ demonstrated that the d-wave gapped state approaches the Fermi energy as the doped carrier increases, which shows a striking similarity with those observed for underdoped cuprate, suggesting that superconductivity can be realized with increasing the carrier concentration (Fig. 32).

Our conclusions are summarized as follows at the present stage:

- ① We can successfully enhance the solubility limit until $x = 0.13$ by using a mechanical alloying method.
- ② The μ SR measurement indicates that there is non-oscillatory signal that indicates the absence of a long-range order below T_N (Fig. 33).
- ③ At around $x = 0.1$, the Griffith phase (short-range A.F clusters) appears to grow upon cooling in the paramagnetic phase.
- ④ Magnetic susceptibility becomes dramatically suppressed with more fluorine substitution at an apical oxygen site.

In conclusion, however, we can not get a bulk superconductivity, probably due to insufficient carriers in the IrO_2 planes.

Acknowledgements

I deeply acknowledge my colleagues, Drs. H. Sawa, M. Uehara, T. Muranaka, Y. Zenitani, S. Akutagawa, K. Kawashima, K. Horigane, Z.A. Ren, S. Kuroiwa, N. Kase and all our members in my laboratory for our collaborations. In particular, I deeply acknowledge Dr. Kumakura for the discussion of applications of MgB_2 . Finally, we thank to K. Horigane, M. Akimitsu, E. Sakamoto and H. Tanaka for assisting me to prepare the manuscript.

References

- 1) Noma, S., Saito, T., Ekino, T., Akimitsu, J. and Sueno, S. (1993) Superconducting phase in $\text{Nb}_{1-x}\text{Ta}_x\text{Se}_3$ ($0.135 < x < 0.16$). *Phys. Rev. B* **48**, 9620–9627.
- 2) Kawabata, K. (1985) Impurity effects on superconductivity and charge density waves in NbSe_3 . *J. Phys. Soc. Jpn.* **54**, 762–770.
- 3) Bednorz, J.G. and Müller, K.A. (1986) Possible high- T_c superconductivity in the Ba-La-Cu-O system. *Z. Phys. B* **64**, 189–193.
- 4) Wu, M.K., Ashburn, J.R., Torng, C.J., Hor, P.H., Meng, R.L., Gao, L. *et al.* (1987) Superconductivity at 93 K in a new mixed-phase Y-Ba-Cu-O compound system at ambient pressure. *Phys. Rev. Lett.* **58**, 908–910.
- 5) Akimitsu, J., Yamazaki, A., Sawa, H. and Fujiki, H. (1987) Superconductivity in the Bi-Sr-Cu-O system. *Jpn. J. Appl. Phys.* **26**, L2080–L2081.
- 6) Akimitsu, J. (1988) Superconducting and physical properties of Bi-Sr-Cu-O system. *Jpn. J. Appl. Phys. Ser. 1 Supercond. Mater.* 19–23.
- 7) Maeda, H., Tanaka, Y., Fukutomi, M. and Asano, T. (1988) A new high- T_c oxide superconductor without a rare earth element. *J. Appl. Phys.* **27**, L209–L210.
- 8) Akimitsu, J., Suzuki, S., Watanabe, M. and Sawa, H. (1988) Superconductivity in the Nd-Sr Ce-Cu-O system. *Jpn. J. Appl. Phys.* **27**, L1859–L1860.
- 9) Sawa, H., Suzuki, S., Watanabe, M., Akimitsu, J., Matsubara, H., Watabe, H. *et al.* (1989) Unusually simple crystal structure of an Nd-Ce-Sr-Cu-O superconductor. *Nature* **337**, 347–348.
- 10) Tokura, Y., Takagi, H. and Uchida, S. (1989) A superconducting copper oxide compound with electrons as the charge carriers. *Nature* **337**, 345–347.
- 11) Tokura, Y. and Arima, T. (1990) New classification method for layered copper compounds and its application to design of new high T_c superconductors. *Jpn. J. Appl. Phys.* **29**, 2388–2402.
- 12) Miyazaki, Y., Yamane, H., Kajitani, T., Oku, T., Hiraga, K., Morii, Y. *et al.* (1992) Preparation and crystal structure of $\text{Sr}_2\text{CuO}_2(\text{CO}_3)$. *Physica C* **191**, 434–440.
- 13) Uehara, M., Nakata, H. and Akimitsu, J. (1993) Superconductivity in the new compound $\text{Sr}_2\text{CuO}_2(\text{CO}_3)_{1-x}(\text{BO}_3)_x$. *Physica C* **216**, 453–457.
- 14) Nakata, H., Uehara, M., Akimitsu, J. and Matsui, Y. (1994) A new family of superconductors containing carbonate group. *Bull. Electrotech. Lab.* **58**, 468–472.
- 15) Uehara, M., Uoshima, M., Ishiyama, S., Nakata, H., Akimitsu, J., Matsui, Y. *et al.* (1994) A new homologous series of oxycarbonate superconductors $\text{Sr}_2(\text{Ca,Sr})_{n-1}\text{Cu}_n(\text{CO}_3)_{1-x}(\text{BO}_3)_x\text{O}_y$ ($n = 1, 2$ and 3). *Physica C* **229**, 310–314.
- 16) Azuma, M., Hiroi, Z., Takano, M., Ishida, K. and Kitaoka, Y. (1994) Observation of a spin gap in SrCu_2O_3 comprising spin-1/2 quasi-1D two-leg ladders. *Phys. Rev. Lett.* **73**, 3463–3466.
- 17) Rice, T.M., Gopalan, S. and Sigrist, M. (1993) Superconductivity, spin gaps and luttinger liquids in a class of cuprates. *Europhys. Lett.* **23**, 445–449.
- 18) Dagotto, E., Riera, J. and Scalapino, D. (1992) Superconductivity in ladders and coupled planes. *Phys. Rev. B* **45**, 5744–5747.
- 19) Uehara, M., Nagata, T., Akimitsu, J., Takahashi, H., Mori, N. and Kinoshita, K. (1996) Superconductivity in the new family of superconductors containing carbonate group. *Bull. Electrotech. Lab.* **58**, 468–472.

- tivity in the ladder material $\text{Sr}_{0.4}\text{Ca}_{13.6}\text{Cu}_{24}\text{O}_{41.84}$. *J. Phys. Soc. Jpn.* **65**, 2764–2767.
- 20) Nagata, T., Uehara, M., Goto, J., Akimitsu, J., Motoyama, N., Eisaki, H. *et al.* (1998) Pressure-induced dimensional crossover and superconductivity in the hole-doped two-leg ladder compound $\text{Sr}_{14-x}\text{Ca}_x\text{Cu}_{24}\text{O}_{41}$. *Phys. Rev. Lett.* **81**, 1090–1093.
 - 21) Nagamatsu, J., Nakagawa, N., Muranaka, T., Zenitani, Y. and Akimitsu, J. (2001) Superconductivity at 39K in magnesium diboride. *Nature* **410**, 63–64.
 - 22) Kortus, J., Mazin, I.I., Belashchenko, K.D., Antropov, V.P. and Boyer, L.L. (2001) Superconductivity of metallic boron in MgB_2 . *Phys. Rev. Lett.* **86**, 4656–4659.
 - 23) Kumakura, H. (2012) Development of high performance MgB_2 tapes and wires. *J. Phys. Soc. Jpn.* **81**, 011010.
 - 24) Giunchi, G., Ceresara, S., Ripamonti, G., Di Zenobio, A., Rossi, S., Chiarelli, S. *et al.* (2003) High performance new MgB_2 superconducting hollow wires. *Supercond. Sci. Technol.* **16**, 285–291.
 - 25) Amano, G., Akutagawa, S., Muranaka, T., Zenitani, Y. and Akimitsu, J. (2004) Superconductivity at 18K in yttrium sesquicarbide system, Y_2C_3 . *J. Phys. Soc. Jpn.* **73**, 530–532.
 - 26) Akutagawa, S. and Akimitsu, J. (2007) Superconductivity of Y_2C_3 by specific heat measurement. *J. Phys. Soc. Jpn.* **76**, 024713.
 - 27) Akutagawa, S., Ohashi, T., Kitano, H., Maeda, A. and Akimitsu, J. (2007) Microwave electrical resistivity of moderately high T_c superconductor, Y_2C_3 . *Physica C* **460–462**, 649–650.
 - 28) Krupka, M.C., Giorgi, A.L., Krikorian, N.H. and Szklart, E.G. (1969) High pressure synthesis and superconducting properties of yttrium sesquicarbide. *J. Less Common Met.* **17**, 91–98.
 - 29) Harada, A., Akutagawa, S., Miyamichi, Y., Mukuda, H., Kitaoka, Y. and Akimitsu, J. (2007) Multigap superconductivity in Y_2C_3 : A ^{13}C -NMR study. *J. Phys. Soc. Jpn.* **76**, 023704.
 - 30) Kuroiwa, S., Saura, Y., Akimitsu, J., Hiraishi, M., Miyazaki, M., Satoh, K.H. *et al.* (2008) Multigap superconductivity in sesquicarbides La_2C_3 and Y_2C_3 . *Phys. Rev. Lett.* **100**, 097002.
 - 31) Ekimov, E.A., Sidorov, V.A., Bauer, E.D., Mel'nik, N.N., Curro, N.J., Thompson, J.D. *et al.* (2004) Superconductivity in diamond. *Nature* **428**, 542–545.
 - 32) Takano, Y., Nagao, M., Sakaguchi, I., Tachiki, M. and Hatano, T. (2004) Superconductivity in diamond thin films well above liquid helium temperature. *Appl. Phys. Lett.* **85**, 2851–2853.
 - 33) Bustarret, E., Marcenat, C., Achatz, P., Kacmarcik, J., Levy, F., Huxley, A. *et al.* (2006) Superconductivity in doped cubic silicon. *Nature* **444**, 465–468.
 - 34) Fukuyama, H. (2006) High-temperature superconductivity by transforming bonds into bands. *J. Supercond. Novel Mag.* **19**, 201–202.
 - 35) Ren, Z.A., Kato, J., Muranaka, T., Akimitsu, J., Kriener, M. and Maeno, Y. (2007) Superconductivity in boron-doped SiC. *J. Phys. Soc. Jpn.* **76**, 103710.
 - 36) Muranaka, T., Kikuchi, Y., Yoshizawa, T., Shirakawa, N. and Akimitsu, J. (2008) Superconductivity in carrier-doped silicon carbide. *Sci. Technol. Adv. Mater.* **9**, 044204.
 - 37) Remeika, J.P., Espinosa, G.P., Cooper, A.S., Barz, H., Rowell, J.M., McWhan, D.B. *et al.* (1980) A new family of ternary intermetallic superconducting/magnetic stannides. *Solid State Commun.* **34**, 923–926.
 - 38) Kase, N., Kittaka, S., Sakakibara, T. and Akimitsu, J. (2012) Superconducting gap structure of the cage compound $\text{Sc}_5\text{Rh}_6\text{Sn}_{18}$. *J. Phys. Soc. Jpn.* **81**, SB016.
 - 39) Volovik, G.E. (1993) Superconductivity with lines of GAP nodes: Density of states in the vortex. *JETP Lett.* **58**, 469–473.
 - 40) Sawa, H., Obara, K., Akimitsu, J., Matsui, Y. and Horiuchi, S. (1989) A new family of superconducting copper oxides: $(\text{Ln}_{1-x}\text{Ce}_x)_2(\text{Ba}_{1-y}\text{Ln}_y)_2\text{Cu}_3\text{O}_{10-\delta}$ (Ln: Nd, Sm, Eu). *J. Phys. Soc. Jpn.* **58**, 2252–2255.
 - 41) Akimitsu, J., Uehara, M., Ogawa, M., Nakata, H., Tomimoto, K., Miyazaki, Y. *et al.* (1992) Superconductivity in the new compound $(\text{Y}_{1-x}\text{Ca}_x)_{0.95}\text{Sr}_{2.05}\text{Cu}_{2.4}(\text{CO}_3)_{0.6}\text{O}_y$. *Physica C* **201**, 320–324.
 - 42) Uehara, M., Nakata, H., Akimitsu, J., Den, T., Kobayashi, T. and Matsui, Y. (1993) Superconductivities in the (Bi,Pb)-oxycarbonate system. *Physica C* **213**, 51–56.
 - 43) Matsui, Y., Ogawa, M., Uehara, M., Nakata, H. and Akimitsu, J. (1993) Incommensurate and commensurate superstructures in the oxycarbonate superconductor $\text{TlSr}_{4-x}\text{Ba}_x\text{Cu}_2(\text{CO}_3)\text{O}_y$ ($x \approx 2$). *Physica C* **217**, 287–293.
 - 44) Uehara, M., Sahoda, S., Nakata, H., Akimitsu, J. and Matsui, Y. (1994) New Hg-based oxycarbonate superconductor $\text{HgBa}_2\text{Sr}_2\text{CuO}_{6+\delta}(\text{CO}_3)$. *Physica C* **222**, 27–32.
 - 45) Akimitsu, J., Uoshima, M., Ishiyama, S., Sato, M., Nakata, H., Uehara, M. *et al.* (1995) New oxycarbonate superconductors $\text{Sr}_2(\text{Ca,Sr})_{n-1}\text{Cu}_n(\text{CO}_3)\text{O}_y$ ($n = 1, 2, 3$) and $\text{Ba}_2\text{Ca}_{n-1}\text{Cu}_2(\text{CO}_3)\text{O}_y$ ($n = 3$). *In Superconductivity and Superconducting Materials Technologies* (ed. Vincenzini, P.). *Advances in Science and Technology*, Vol. 8, Techna, Faenza, pp. 35–40.
 - 46) Zenitani, Y., Inari, K., Sahoda, S., Uehara, M., Akimitsu, J., Kubota, N. *et al.* (1995) Superconductivity in $(\text{Ca,Na})_2\text{CaCu}_2\text{O}_4\text{Cl}_2$ —The new simplest double-layer cuprate with apical chlorine—. *Physica C* **248**, 167–170.
 - 47) Zenitani, Y., Sahoda, S., Akimitsu, J., Kubota, N. and Ayabe, M. (1996) New superconductor with apical bromine $(\text{Ca,A})_2\text{CuO}_2\text{Br}_2$: A = Na, K. *J. Jpn. Soc. Powder Powder Metall.* **43**, 1087–1089 (in Japanese).
 - 48) Tamura, M., Sato, M., Den, T. and Akimitsu, J. (1998) A new superconductor with 1222 structure

- ($\text{Cu}_{1-x}\text{M}_x$) $\text{Sr}_2(\text{Y}_{1-y}\text{Ce}_y)_2\text{Cu}_2\text{O}_\delta$ ($M = \text{Ti, V, Cr, Fe, Co, Ga, Ge, Mo, Ce, W}$ and Re). *Physica C* **33**, 1–10.
- 49) Takagiwa, H., Akimitsu, J., Furukawa, H. and Yoshizawa, H. (2001) Coexistence of superconductivity and (anti-)ferromagnetism in $\text{RuSr}_2\text{YCu}_2\text{O}_8$. *J. Phys. Soc. Jpn.* **70**, 333–336.
- 50) Kawano, A., Mizuta, Y., Takagiwa, H., Muranaka, T. and Akimitsu, J. (2003) The superconductivity in Re-B system. *J. Phys. Soc. Jpn.* **72**, 1724–1728.
- 51) Kawashima, K., Kawano, A., Muranaka, T. and Akimitsu, J. (2006) Superconductivity in $\text{M}_7\text{Re}_{13}\text{X}$ ($M = \text{W, Mo, X} = \text{B, C}$) compounds. *Physica B* **378–380**, 1118–1119.
- 52) Kawashima, K., Muranaka, T., Kousaka, Y., Akutagawa, S. and Akimitsu, J. (2009) Superconductivity in transition metal-silicide W_5Si_3 . *J. Phys. Conf. Ser.* **150**, 052106.
- 53) Kawashima, K., Maruyama, M., Fukuma, M. and Akimitsu, J. (2010) Superconducting state in YSn_3 with a AuCu_3 -type structure. *Phys. Rev. B* **82**, 094517.
- 54) Kase, N., Muranaka, T. and Akimitsu, J. (2008) Superconductivity in the ternary germanide $\text{Y}_3\text{Pt}_4\text{Ge}_6$. *J. Phys. Soc. Jpn.* **77**, 054714.
- 55) Fukuma, M., Kawashima, K., Maruyama, M. and Akimitsu, J. (2011) Superconductivity in W_5SiB_2 with the T_2 phase structure. *J. Phys. Soc. Jpn.* **80**, 024702.
- 56) Fukuma, M., Kawashima, K. and Akimitsu, J. (2012) Superconducting state in $(\text{W,Ta})_5\text{SiB}_2$. *Phys. Procedia* **27**, 48–51.
- 57) Kawashima, K., Inoue, K., Ishikawa, T., Fukuma, M., Yoshikawa, M. and Akimitsu, J. (2012) Superconductivity in $\text{Ba}(\text{TM,Si})_2$ ($\text{TM} = \text{Pd, Pt, Cu, Ag}$ and Au) with AlB_2 -type structure. *J. Phys. Soc. Jpn.* **81**, 4717.
- 58) Miyazaki, S., Kawashima, K., Ipponjima, T., Fukuma, M., Hyakumura, D. and Akimitsu, J. (2013) Superconductivity in KSn_2 with the MgZn_2 -type structure. *J. Korean Phys. Soc.* **63**, 475–476.
- 59) Ipponjima, T., Kawashima, K., Miyazaki, S., Hyakumura, D., Yoshikawa, M. and Akimitsu, J. (2013) New germanide superconductors with the type-I clathrate type structure. *Physica C* **494**, 74–76.
- 60) Kuchida, S., Muranaka, T., Kawashima, K., Inoue, K., Yoshikawa, M. and Akimitsu, J. (2013) Superconductivity in Lu_2SnC . *Physica C* **494**, 77–79.
- 61) Niimura, H., Kawashima, K., Inoue, K., Yoshikawa, M. and Akimitsu, J. (2014) Superconductivity in the ternary boride $\text{Cr}_2\text{Re}_3\text{B}$ with the β -Mn-type structure. *J. Phys. Soc. Jpn.* **83**, 044702.
- 62) Kuroiwa, S., Kawashima, H., Kinoshita, H., Okabe, H. and Akimitsu, J. (2007) Superconductivity in ternary silicide NaAlSi with layered diamond-like structure. *Physica C* **466**, 11–15.
- 63) Drozdov, A.P., Erements, M.I., Troyan, I.A., Ksenofontov, V. and Shylin, S.I. (2015) Conventional superconductivity at 203 kelvin at high pressures in the sulfur hydride system. *Nature* **525**, 73–76.
- 64) Drozdov, A.P., Kong, P.P., Minkov, V.S., Besedin, S.P., Kuzovnikov, M.A., Mozaffari, S. *et al.* (2019) Superconductivity at 250 K in lanthanum hydride under high pressure. *Nature* **569**, 528–531.
- 65) Somayazulu, M., Ahart, M., Mishra, A.K., Geballe, Z.M., Baldini, M., Meng, Y. *et al.* (2019) Evidence for superconductivity above 260 K in lanthanum superhydride at megabar pressure. *Phys. Rev. Lett.* **122**, 027001.
- 66) Watanabe, H., Shirakawa, T. and Yunoki, S. (2013) Monte Carlo study of an unconventional superconducting phase in iridium oxide $J_{\text{eff}} = 1/2$ Mott insulators induced by carrier doping. *Phys. Rev. Lett.* **110**, 027002.
- 67) Yan, Y.J., Ren, M.Q., Xu, H.C., Xie, B.P., Tao, R., Choi, H.Y. *et al.* (2015) Electron-doped Sr_2IrO_4 : An analogue of hole-doped cuprate superconductors demonstrated by scanning tunneling microscopy. *Phys. Rev. X* **5**, 041018.
- 68) Kim, Y.K., Sung, N.H., Denlinger, J.D. and Kim, B.J. (2016) Observation of a d -wave gap in electron-doped Sr_2IrO_4 . *Nat. Phys.* **12**, 37–41.
- 69) Terashima, K., Sunagawa, M., Fujiwara, H., Fukura, T., Fujii, M., Okada, K. *et al.* (2017) Evolution of the remnant Fermi-surface state in the lightly doped correlated spin-orbit insulator $\text{Sr}_{2-x}\text{La}_x\text{IrO}_4$. *Phys. Rev. B* **96**, 041106.
- 70) Horigane, K., Fujii, M., Okabe, H., Kobayashi, K., Horie, R., Ishii, H. *et al.* (2018) Magnetic phase diagram of $\text{Sr}_{2-x}\text{La}_x\text{IrO}_4$ synthesized by mechanical alloying. *Phys. Rev. B* **97**, 064425.
- 71) Terashima, K., Paris, E., Salas-Colera, E., Simonelli, L., Joseph, B., Wakita, T. *et al.* (2018) Determination of the local structure of $\text{Sr}_{2-x}\text{M}_x\text{IrO}_4$ ($M = \text{K, La}$) as a function of doping and temperature. *Phys. Chem. Chem. Phys.* **20**, 23783–23788.

(Received Feb. 5, 2019; accepted Apr. 23, 2019)

Profile

Jun Akimitsu was born in Hiroshima Prefecture in 1939. He graduated from the University of Tokyo and also received a Ph.D. from there. He became Research Associate at Institute for the Solid State Physics (ISSP), the University of Tokyo (1970–1976). He moved to Aoyama Gakuin University as Associate Professor (1976–1982), and later became Professor (1982–2015). He became the Dean of the Center for Advanced Technology, Aoyama Gakuin University (1998–2015). Meanwhile, he was a visiting professor at MIT (U.S.), and Monash University (Australia) and Guest Scientist at Brookhaven National Laboratory. After retirement from Aoyama Gakuin University, he moved to Research Institute for Interdisciplinary Science, Okayama University, in 2015. He is presently Professor (Special Appointment) of Okayama University.



He has received the following Awards; 1) 1997, Superconducting Science and Technology Award (first: For the discovery of Superconductivity in a ladder compound); 2) 1998, Nishina Memorial Award; 3) 2001, Medal with Purple Ribbon; 4) 2002, The Asahi Prize; 5) 2002, Masumoto Hakaru Award; 6) 2002, Superconducting Science and Technology Award (second: For the discovery of MgB_2); 7) 2002, Magnetic Society of Japan Award; 8) 2003, Bernd T. Matthias Prize; 9) 2007, Nishikawa Award; 10) 2008, James C. McGroddy Prize for New Materials; 11) 2012, Special Prize from the Japanese Society for Neutron Society; 12) 2014, The order of the Sacred Treasure; 13) 2019, Superconductivity Science and Technology Award (third: For distinguished contribution to the Discovery of New Superconductors).